

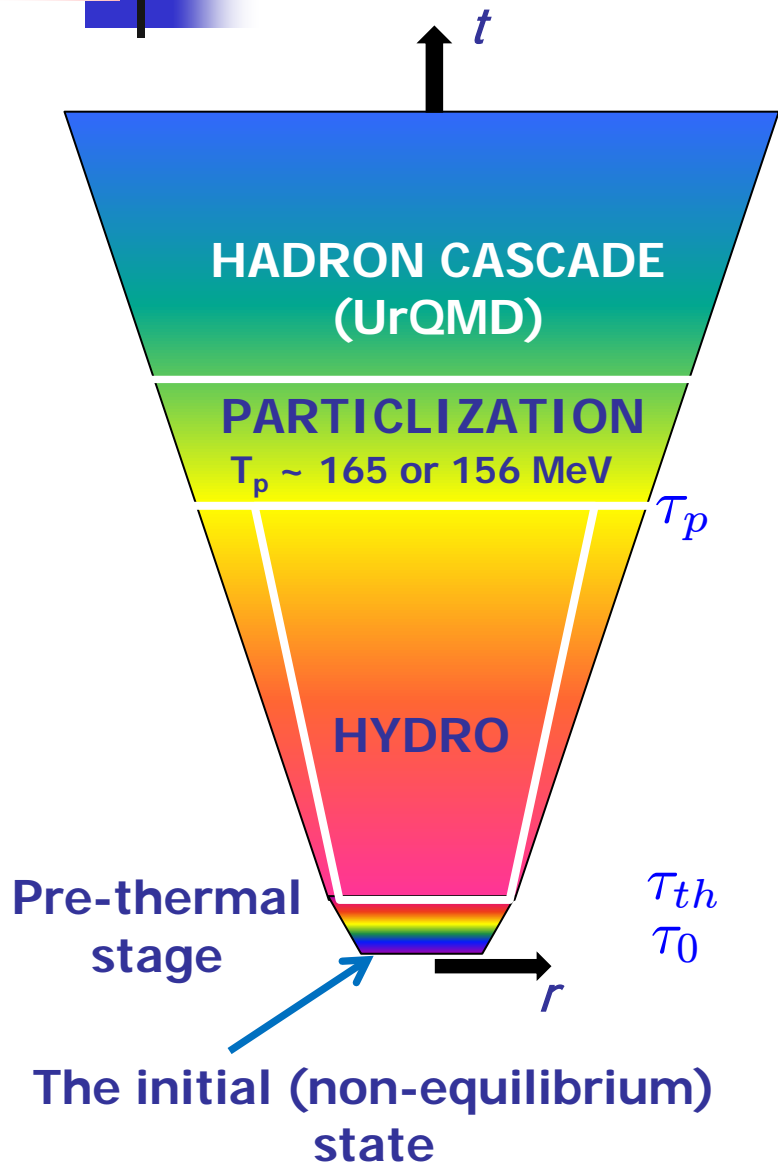
Strange meson probes of dense hadron matter in A+A collisions

Yuri Sinyukov

Bogolyubov Institute, Kiev

NICA DAYS in WARSAW, November 6-10, 2017

Integrated HydroKinetic model: HKM → iHKM



Complete algorithm incorporates the stages:

- generation of the initial states;
- thermalization of initially non-thermal matter;
- viscous chemically equilibrated hydrodynamic expansion;
- sudden (with option: continuous) particlization of expanding medium;
- a switch to UrQMD cascade with near equilibrium hadron gas as input;
- simulation of observables.

Yu.S., Akkelin, Hama: PRL 89 (2002) 052301;

... + Karpenko: PRC 78 (2008) 034906;

Karpenko, Yu.S. : PRC 81 (2010) 054903;

... PLB 688 (2010) 50;

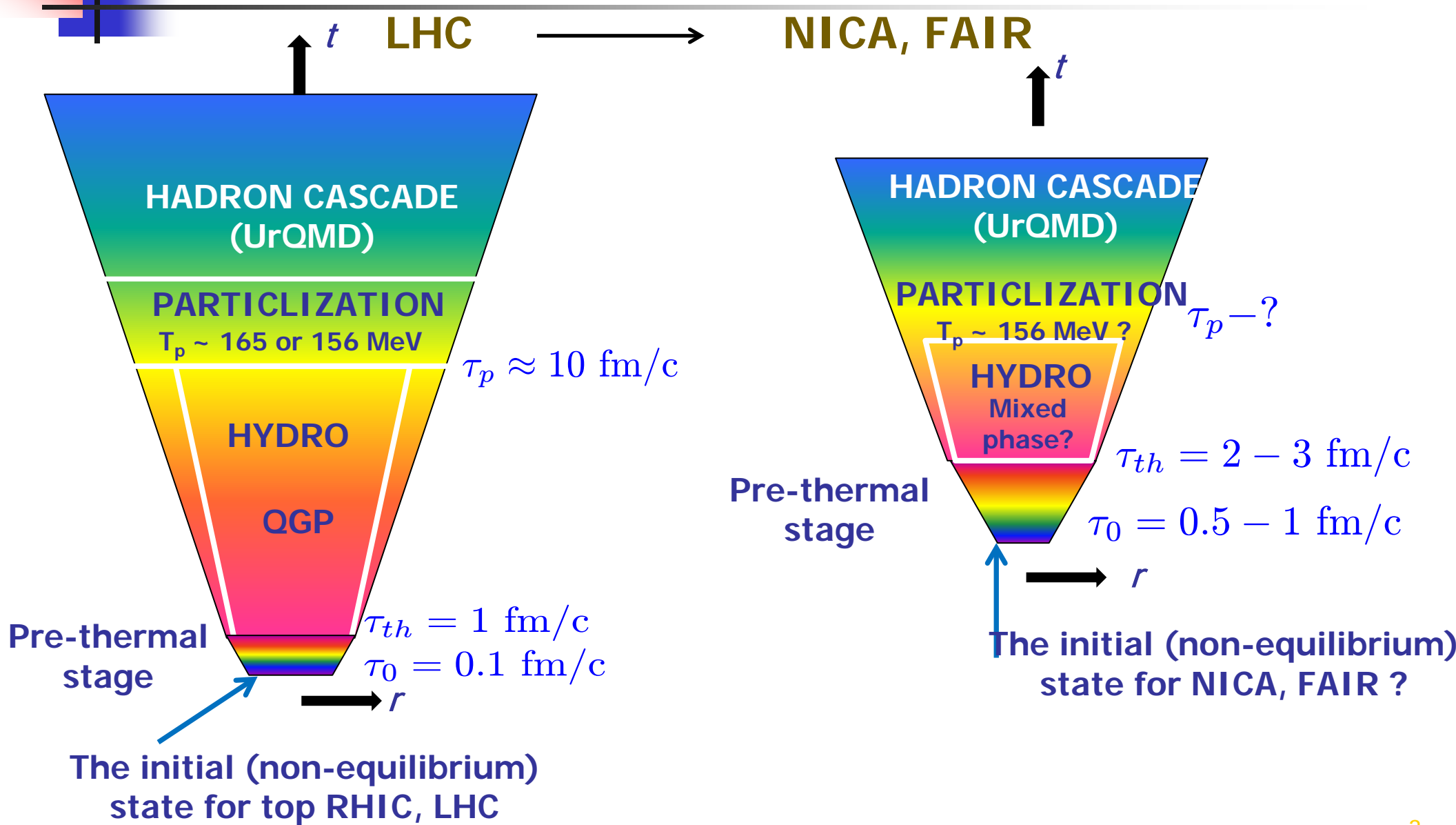
Akkelin, Yu.S. : PRC 81 (2010) 064901;

Karpenko, Yu.S., Werner: PRC 87 (2013) 024914;

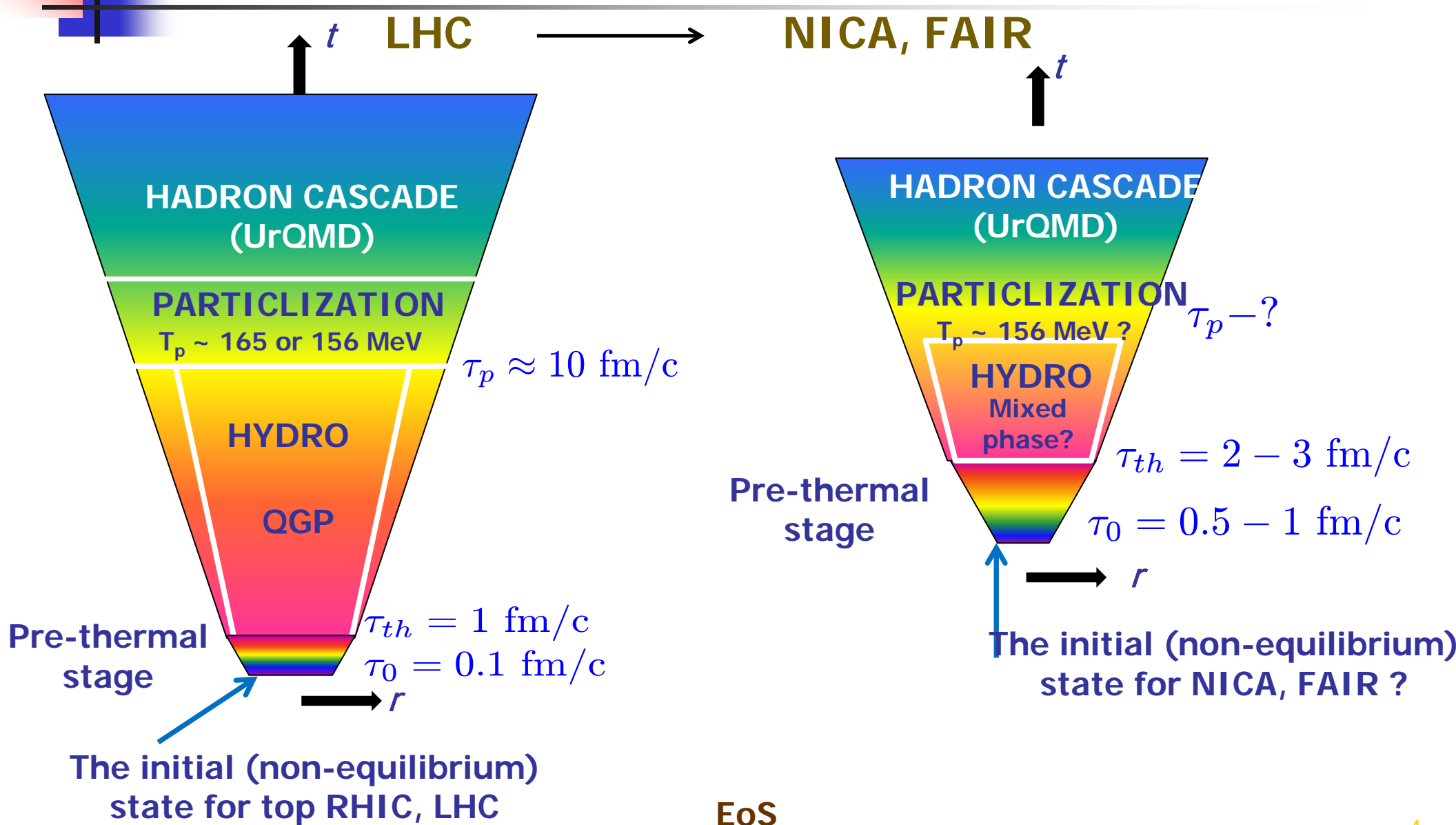
Naboka, Akkelin, Karpenko, Yu.S. : PRC **91** (2015) 014906;

Naboka, Karpenko, Yu.S. Phys. Rev. C **93** (2016) 024902.

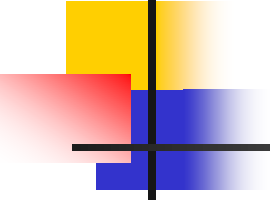
Space-time picture of A+A collisions:



Space-time picture of A+A collisions:



Small (zero) baryon chemical potentials → Large baryon chemical potentials



Initial states

The most commonly used models of initial state are:

High Energies

MC-G (Monte Carlo Glauber)
MC-KLN (Monte Carlo Kharzeev-Levin-Nardi)
EPOS (parton-based Gribov-Regge model)
EKRT (perturbative QCD + saturation model)
IP-Glasma (Impact Parameter dependent Glasma)

Low Energies

MC-G (Monte Carlo Glauber) - ?
UrQMD (Ultra-Relativistic Molecular Dynamics) - ?

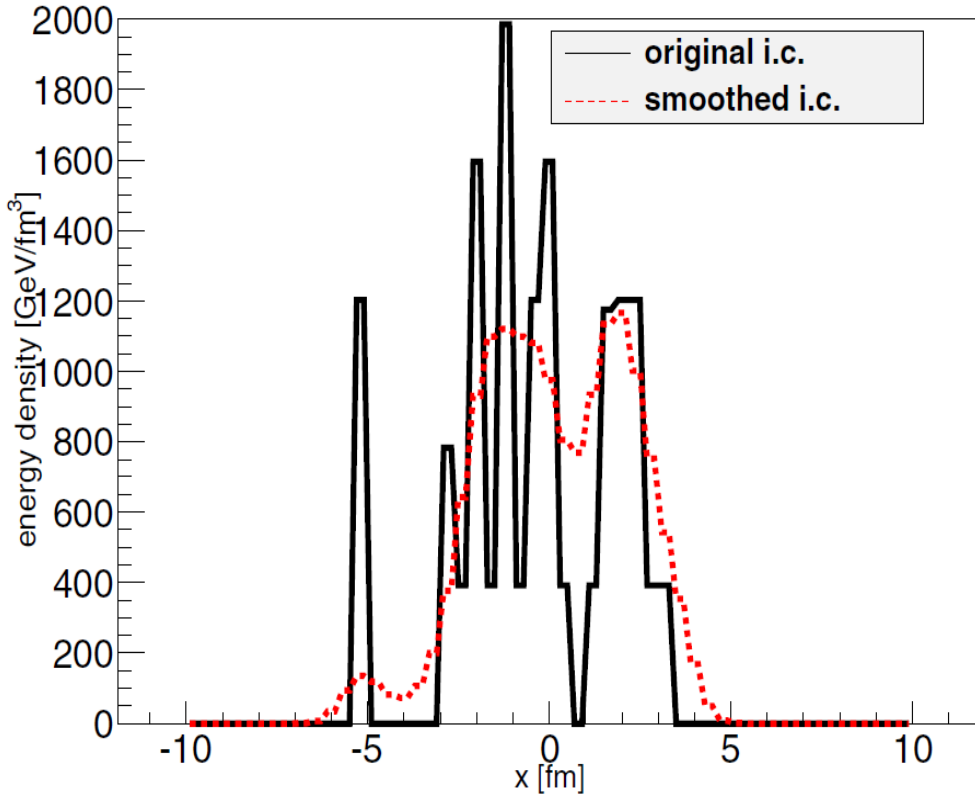
PROBLEM:

**No one model leads to the proper matter thermalization,
while**

**the biggest experimental discovery for a few decades is that hydrodynamics is the basis
of the "Standard Model " of high energy A+A collisions**

MC-G Initial State (IS) attributed to $\tau_0 = 0.1 \text{ fm}/c$

GLISSANDO 2



- The initial state (IS) is highly inhomogeneous.
- It is not locally equilibrated.
- The IS most probable is strongly momentum anisotropic (result from CGC)

$$f(t_{\sigma_0}, \mathbf{r}_{\sigma_0}, \mathbf{p}) = \epsilon(b; \tau_0, \mathbf{r}_T) f_0(p)$$

$$T_0^{\mu\nu}(x) = \int d^3p \frac{p^\mu p^\nu}{p_0} f_{\sigma_0}(x, p); T^{00}[f_0(p)] = 1$$

$$f_0^*(p) \propto \exp\left(-\sqrt{\frac{p_T^2}{\lambda_\perp^2} + \frac{p_L^2}{\lambda_\parallel^2}}\right) \quad \text{Florkowski et al}$$

MC-G Hybrid for ensemble of ISs :

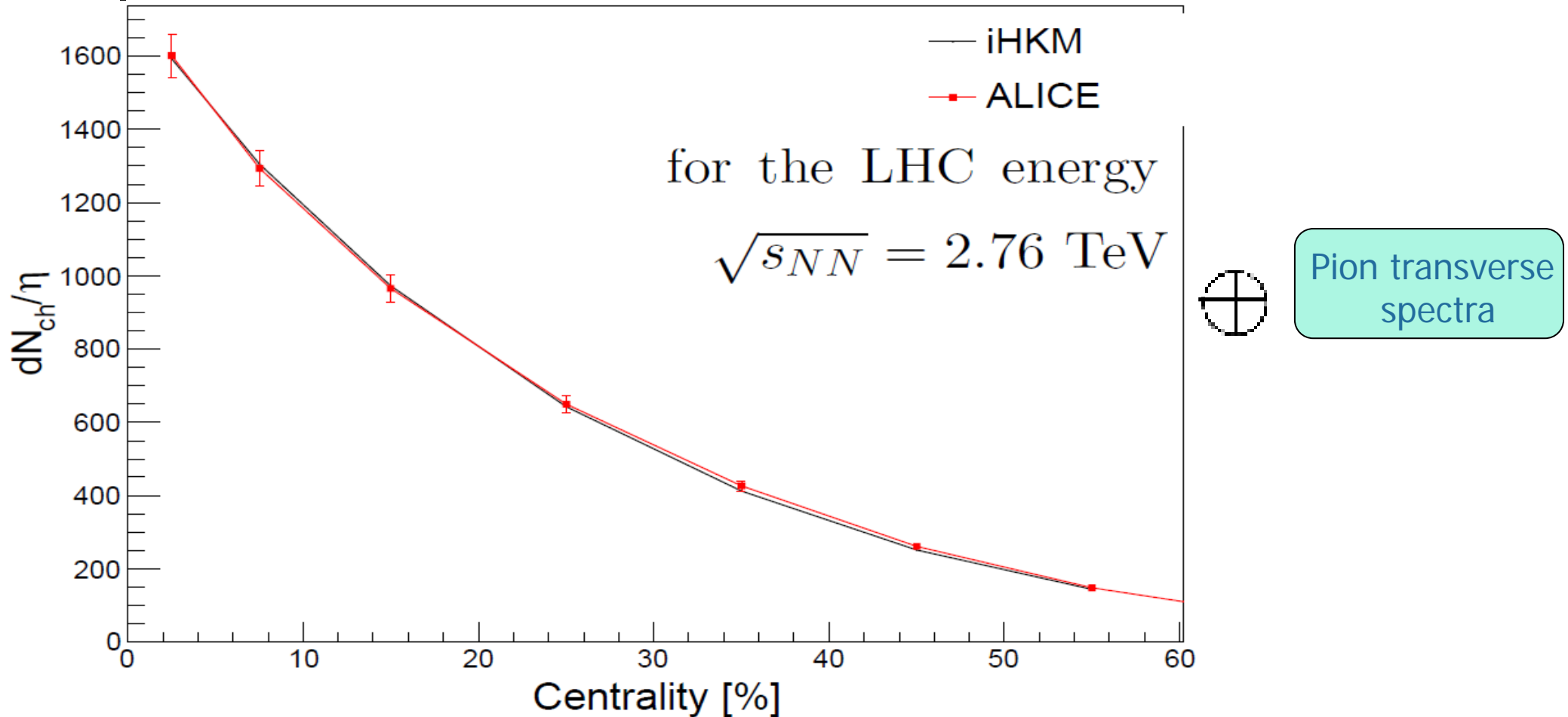
Parameters of IS

$$\epsilon(b; \tau_0, \mathbf{r}_T) = \epsilon_0 \frac{(1 - \alpha) N_W(b, \mathbf{r}_T)/2 + \alpha N_{bin}(b, \mathbf{r}_T)}{(1 - \alpha) N_W(b = 0, \mathbf{r}_T = 0)/2 + \alpha N_{bin}(b = 0, \mathbf{r}_T = 0)}$$

$$\Lambda = \lambda_\perp / \lambda_\parallel$$

$$\epsilon_0, \alpha = 0.24$$

Multiplicity dependence of all charged particles on centrality



parameter values: $\alpha = 0.24, \tau_{th} = 1\text{fm}/c, \epsilon_0 = f(\tau_0, \tau_{rel}, \eta/s, \Lambda, \text{EoS} \rightarrow T_{ch} \approx T_h)$

Pre-thermal stage (thermalization)

Akkelin, Yu.S. :PRC **81** (2010); Naboka, Akkelin, Karpenko, Yu.S. : PRC **91** (2015).

Non-thermal state at τ_0



locally near equilibrated state at τ_{th}

Boltzmann equation in
relaxation time approximation
(integral form)

MAIN OBJECT

$$\mathcal{P}_\sigma(x, p) = \exp\left(-\int_t^{t_\sigma} \frac{d\bar{t}}{\tau_{rel}(\bar{x}, p)}\right)$$
$$\bar{x} \equiv (\bar{t}, \mathbf{x}_\sigma + (\mathbf{p}/p_0)(\bar{t} - t_\sigma))$$

Pre-thermal stage (thermalization)

Akkelin, Yu.S. :PRC **81** (2010); Naboka, Akkelin, Karpenko, Yu.S. : PRC **91** (2015).

Non-thermal state $\tau_0 = 0.1 \text{ fm}/c \longrightarrow$ locally near equilibrated state $\tau_{th} = 1 \text{ fm}/c$

Boltzmann equation in
relaxation time approximation
(integral form)

MAIN OBJECT

$$\mathcal{P}_\sigma(x, p) = \exp\left(-\int_t^{t_\sigma} \frac{d\bar{t}}{\tau_{rel}(\bar{x}, p)}\right)$$

$$\bar{x} \equiv (\bar{t}, \mathbf{x}_\sigma + (\mathbf{p}/p_0)(\bar{t} - t_\sigma))$$

MAIN ANSATZ with minimal number of parameters: $\tau_0, \tau_{th}, \tau_{rel}$

$$\mathcal{P}_{\tau_0 \rightarrow \tau}(\tau) = \left(\frac{\tau_{th} - \tau}{t_{th} - \tau_0} \right)^{\frac{\tau_{th} - \tau_0}{\tau_{rel}(\tau_0)}} \longrightarrow T^{\mu\nu}(x) = T_{\text{free}}^{\mu\nu}(x)\mathcal{P}(\tau) + T_{\text{hyd}}^{\mu\nu}(x)(1 - \mathcal{P}(\tau))$$

$$\longrightarrow 0 \leq \mathcal{P}(\tau) \leq 1, \mathcal{P}(\tau_0) = 1, \mathcal{P}(\tau_{th}) = 0, \partial_\mu \mathcal{P}(\tau)_{\tau_{th}} = 0$$

Pre-thermal stage (thermalization)

Akkelin, Yu.S. :PRC **81** (2010); Naboka, Akkelin, Karpenko, Yu.S. : PRC **91** (2015).

Non-thermal state $\tau_0 = 0.1 \text{ fm}/c \longrightarrow$ locally near equilibrated state $\tau_{th} = 1 \text{ fm}/c$

Boltzmann equation in
relaxation time approximation
(integral form)

MAIN OBJECT

$$\mathcal{P}_\sigma(x, p) = \exp\left(-\int_t^{t_\sigma} \frac{d\bar{t}}{\tau_{rel}(\bar{x}, p)}\right)$$

$$\bar{x} \equiv (\bar{t}, \mathbf{x}_\sigma + (\mathbf{p}/p_0)(\bar{t} - t_\sigma))$$

MAIN ANSATZ with minimal number of parameters: $\tau_0, \tau_{th}, \tau_{rel}$

$$\mathcal{P}_{\tau_0 \rightarrow \tau}(\tau) = \left(\frac{\tau_{th} - \tau}{t_{th} - \tau_0}\right)^{\frac{\tau_{th} - \tau_0}{\tau_{rel}(\tau_0)}} \longrightarrow T^{\mu\nu}(x) = T_{\text{free}}^{\mu\nu}(x)\mathcal{P}(\tau) + T_{\text{hyd}}^{\mu\nu}(x)(1 - \mathcal{P}(\tau))$$

$$\longrightarrow 0 \leq \mathcal{P}(\tau) \leq 1, \mathcal{P}(\tau_0) = 1, \mathcal{P}(\tau_{th}) = 0, \partial_\mu \mathcal{P}(\tau)_{\tau_{th}} = 0$$

MAIN EQUATIONS

$$\partial_{;\mu} \tilde{T}_{\text{hyd}}^{\mu\nu}(x) = -T_{\text{free}}^{\mu\nu}(x) \partial_{;\mu} \mathcal{P}(\tau)$$

where $\begin{cases} \tilde{T}_{\text{hyd}}^{\mu\nu} = [1 - \mathcal{P}(\tau)] T_{\text{hyd}}^{\mu\nu} \\ \tilde{\pi}^{\mu\nu} = \pi^{\mu\nu} (1 - \mathcal{P}) \end{cases}$

$$(1 - \mathcal{P}(\tau)) \left\langle u^\gamma \partial_{;\gamma} \frac{\tilde{\pi}^{\mu\nu}}{(1 - \mathcal{P}(\tau))} \right\rangle = -\frac{\tilde{\pi}^{\mu\nu} - (1 - \mathcal{P}(\tau)) \pi_{\text{NS}}^{\mu\nu}}{\tau_\pi} - \frac{4}{3} \tilde{\pi}^{\mu\nu} \partial_{;\gamma} u^\gamma$$

The other stages: Hydro evolution, particlization, hadronic cascade

- **Hydro evolution:** $\tau \leq \tau_{th}$ $T^{\mu\nu}(x) = T_{\text{free}}^{\mu\nu}(x)\mathcal{P}(\tau) + T_{\text{hyd}}^{\mu\nu}(x)(1 - \mathcal{P}(\tau)) \xrightarrow{\tau \geq \tau_{th}} T_{\text{hyd}}^{\mu\nu}(x)$
 $= (\epsilon_{\text{hyd}}(x) + p_{\text{hyd}}(x) + \Pi)u_{\text{hyd}}^{\mu}(x)u_{\text{hyd}}^{\nu}(x) - (p_{\text{hyd}}(x) + \Pi)g^{\mu\nu} + \pi^{\mu\nu}.$

IC is the result of pre-thermal evolution reached at τ_{th}

Solving of Israel-Stewart Relativistic Viscous Fluid Dynamics with $\Pi=0$

The other stages: Hydro evolution, particlization, hadronic cascade

$$\tau \geq \tau_{th}$$

- Hydro evolution:** $\tau \leq \tau_{th}$

$$T^{\mu\nu}(x) = T_{\text{free}}^{\mu\nu}(x)\mathcal{P}(\tau) + T_{\text{hyd}}^{\mu\nu}(x)(1 - \mathcal{P}(\tau)) \rightarrow T_{\text{hyd}}^{\mu\nu}(x)$$

$$= (\epsilon_{\text{hyd}}(x) + p_{\text{hyd}}(x) + \Pi)u_{\text{hyd}}^{\mu}(x)u_{\text{hyd}}^{\nu}(x) - (p_{\text{hyd}}(x) + \Pi)g^{\mu\nu} + \pi^{\mu\nu}.$$

Solving of Israel-Stewart Relativistic Viscous Fluid Dynamics with $\Pi=0$

- Particlization:**

at the isotherm hypersurface $T=165$ MeV

energy density $\epsilon = 0.5$ GeV/fm³ for the Laine-Schroeder EoS

Switching hypersurface build with help of Cornelius routine.

For particle distribution the Grad's 14 momentum ansatz is used:

$$\frac{d^3 \Delta N_i}{dp^* d(\cos\theta) d\phi} = \frac{\Delta \sigma_{\mu}^* p^{*\mu}}{p^{*0}} p^{*2} f_{eq}(p^{*0}; T, \mu_i) \left[1 + (1 \mp f_{eq}) \frac{p_{\mu}^* p_{\nu}^* \pi^{*\mu\nu}}{2T^2(\epsilon + p)} \right]$$

The other stages: Hydro evolution, particlization, hadronic cascade

- Hydro evolution:** $\tau \leq \tau_{th}$ $T^{\mu\nu}(x) = T_{\text{free}}^{\mu\nu}(x)\mathcal{P}(\tau) + T_{\text{hyd}}^{\mu\nu}(x)(1 - \mathcal{P}(\tau)) \xrightarrow{\tau \geq \tau_{th}} T_{\text{hyd}}^{\mu\nu}(x)$
 $= (\epsilon_{\text{hyd}}(x) + p_{\text{hyd}}(x) + \Pi)u_{\text{hyd}}^{\mu}(x)u_{\text{hyd}}^{\nu}(x)$
 $- (p_{\text{hyd}}(x) + \Pi)g^{\mu\nu} + \pi^{\mu\nu}.$

Solving of Israel-Stewart Relativistic Viscous Fluid Dynamics with $\Pi=0$

- Particlization:** at the isotherm hypersurface $T=165$ MeV
energy density $\epsilon = 0.5$ GeV/fm³ for the Laine-Schroeder EoS
Switching hypersurface build with help of Cornelius routine.

For particle distribution the Grad's 14 momentum ansatz is used:

$$\frac{d^3 \Delta N_i}{dp^* d(\cos\theta) d\phi} = \frac{\Delta \sigma_{\mu}^* p^{*\mu}}{p^{*0}} p^{*2} f_{eq}(p^{*0}; T, \mu_i) \left[1 + (1 \mp f_{eq}) \frac{p_{\mu}^* p_{\nu}^* \pi^{*\mu\nu}}{2T^2(\epsilon + p)} \right]$$

- Hadronic cascade:** The above distribution function with Poisson distributions for each sort of particle numbers is the input for UrQMD cascade.

The other stages: Hydro evolution, particlization, hadronic cascade

$$\tau \geq \tau_{th}$$

- Hydro evolution:** $\tau \leq \tau_{th}$

$$T^{\mu\nu}(x) = T_{\text{free}}^{\mu\nu}(x)\mathcal{P}(\tau) + T_{\text{hyd}}^{\mu\nu}(x)(1 - \mathcal{P}(\tau)) = T_{\text{hyd}}^{\mu\nu}(x)$$

$$= (\epsilon_{\text{hyd}}(x) + p_{\text{hyd}}(x) + \Pi)u_{\text{hyd}}^{\mu}(x)u_{\text{hyd}}^{\nu}(x)$$

$$- (p_{\text{hyd}}(x) + \Pi)g^{\mu\nu} + \pi^{\mu\nu}.$$

Solving of Israel-Stewart Relativistic Viscous Fluid Dynamics with $\Pi = 0$

- Particlization:**

at the isotherm hypersurface $T=165$ MeV

energy density $\epsilon = 0.5$ GeV/fm³ for the Laine-Schroeder EoS

Switching hypersurface build with help of Cornelius routine.

For particle distribution
the Grad's 14
momentum ansatz is
used:

$$\frac{d^3 \Delta N_i}{dp^* d(\cos\theta) d\phi} = \frac{\Delta \sigma_{\mu}^* p^{*\mu}}{p^{*0}} p^{*2} f_{eq}(p^{*0}; T, \mu_i) \left[1 + (1 \mp f_{eq}) \frac{p_{\mu}^* p_{\nu}^* \pi^{*\mu\nu}}{2T^2(\epsilon + p)} \right]$$

- Hadronic cascade:** The above distribution function with Poisson distributions for each sort of particle numbers is the input for UrQMD

Details are in: Naboka, Karpenko, Yu.S. C **93** (2016) 024902

The iHKM parameters at Laine-Shroeder EoS

The $\frac{dN_{ch}}{d\eta}(c)$ is OK at fixed relative contribution of binary collision $\alpha = 0.24$.

but at different max initial energy densities
when other parameters change:

The two values of the shear viscosity
to entropy is used for comparison:

$$\eta/s = 0.08 \approx \frac{1}{4\pi} \text{ and } \eta/s = 0.2$$

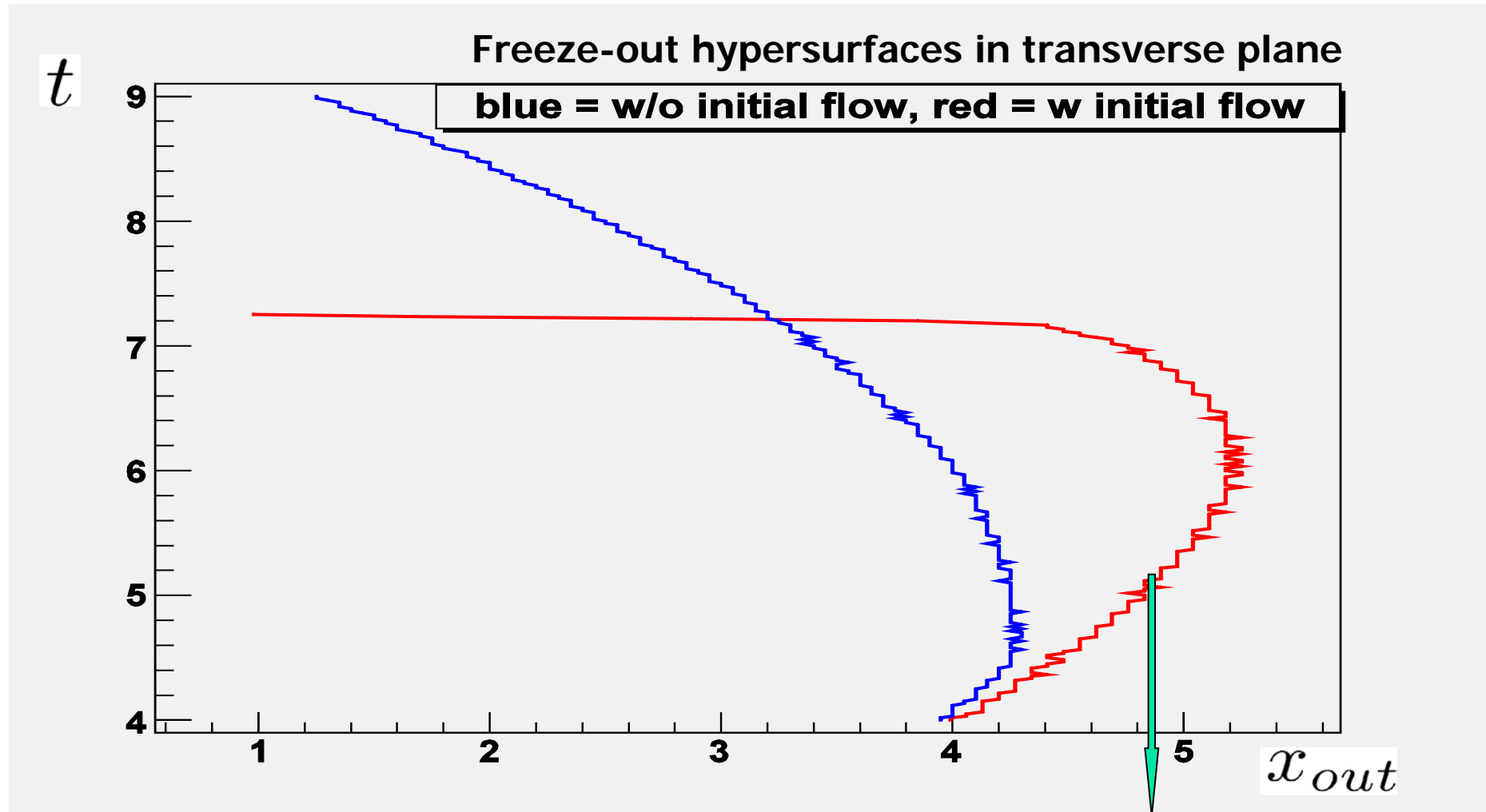
The basic result (selected by red) is
compared with results at other
parameters, including viscous and ideal
pure thermodynamic scenarios
(starting at τ_0 without pre-thermal stage
but with subsequent hadronic cascade).

Model	Λ	τ_{rel}	η/S	τ_0	$\langle \frac{\chi^2}{ndf} \rangle$	ϵ_0 (GeV/fm ³)
Hydro			0	0.1	5.16	1076.5
Hydro			0.08	0.1	6.93	738.8
iHKM	1	0.25	0.08	0.1	3.35	799.5
iHKM	100	0.25	0.08	0.1	3.28	678.8
iHKM	100	0.75	0.08	0.1	3.52	616.5
iHKM	100	0.25	0.2	0.1	6.61	596.9
iHKM	100	0.25	0.08	0.5	5.36	126.7

The values τ_0, τ_{rel} correspond to fm/c.

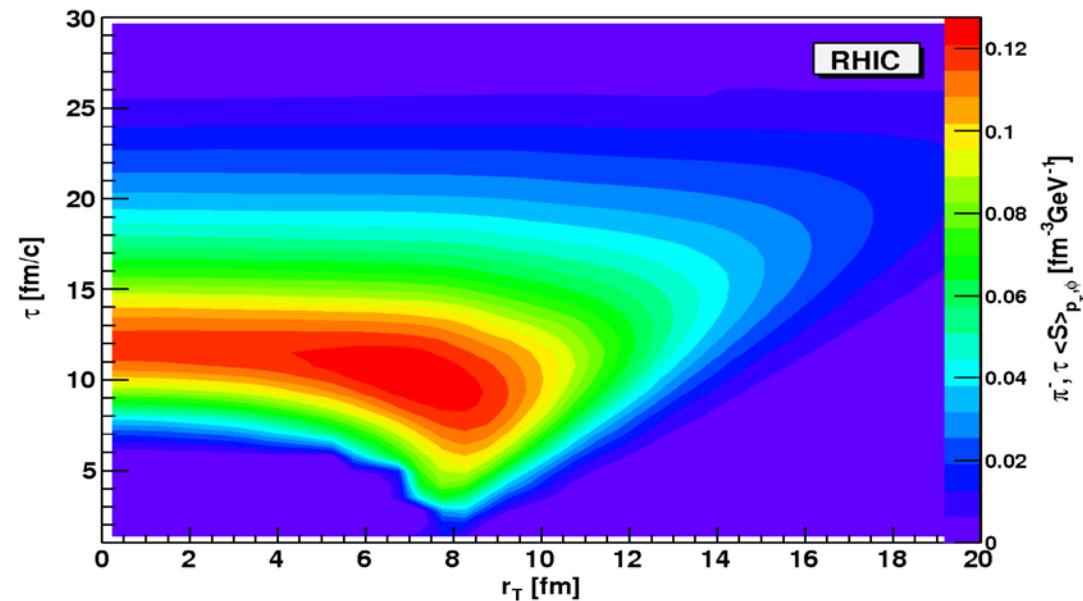
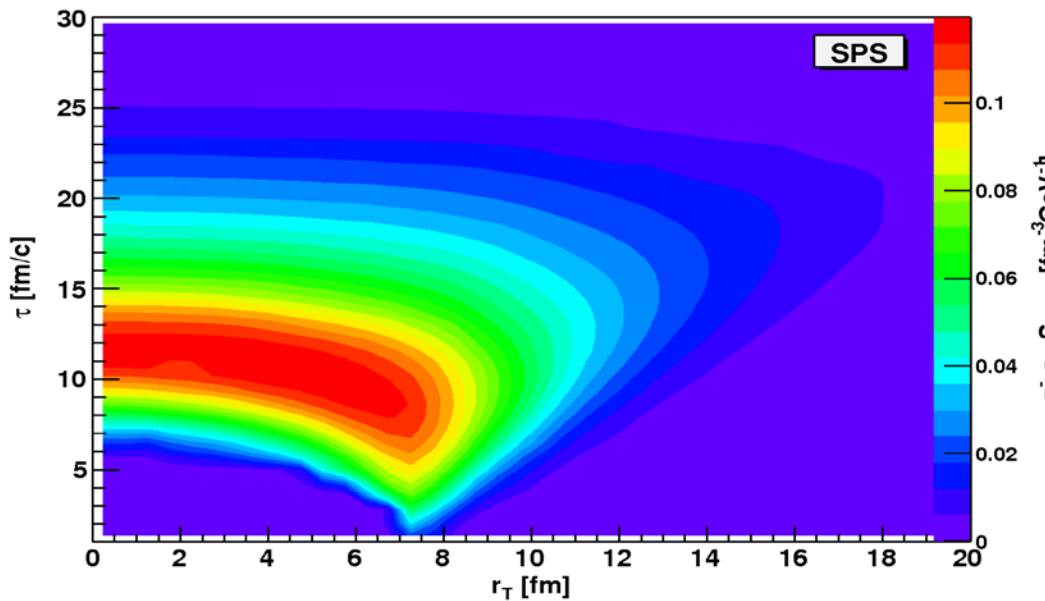
No dramatic worsening of the results
happens if simultaneously with changing
of parameters/scenarios renormalize maximal
initial energy density.

A few principal results from HKM/iHKM on the
correlation femtoscopy

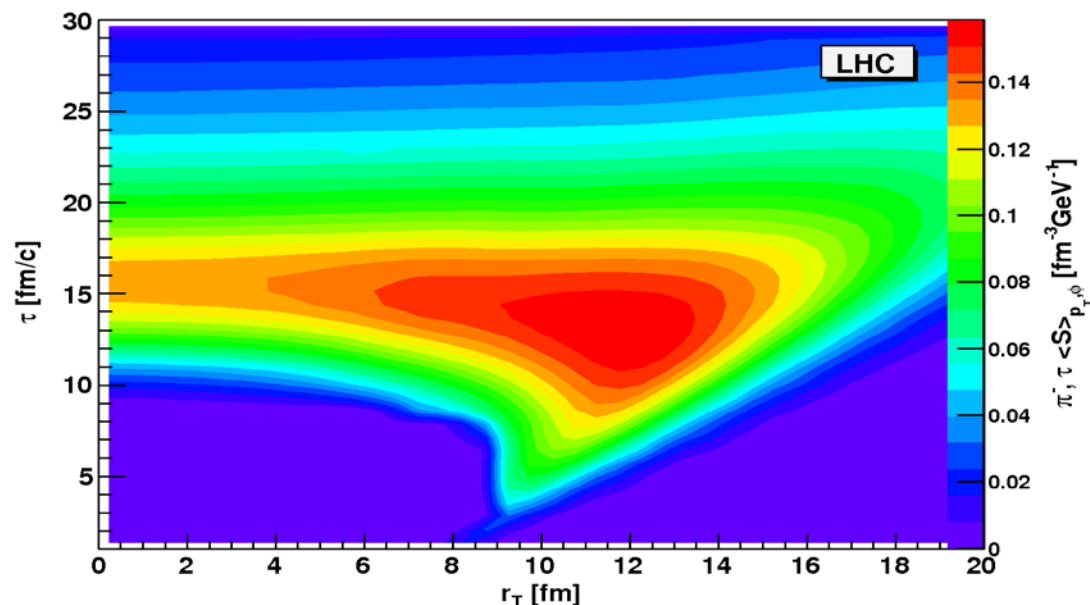


$$R_{out}^2 \approx R_{side}^2 + v^2 \langle \Delta t^2 \rangle_p - 2v \langle \Delta x_{out} \Delta t \rangle_p, v = \frac{p_T}{p_0}$$

Emission functions for top SPS, RHIC and LHC energies



$$R_{out}^2 \approx R_{side}^2 + v^2 \langle \Delta t^2 \rangle_p - 2v \langle \Delta x_{out} \Delta t \rangle_p, v = \frac{p_T}{p^0}$$



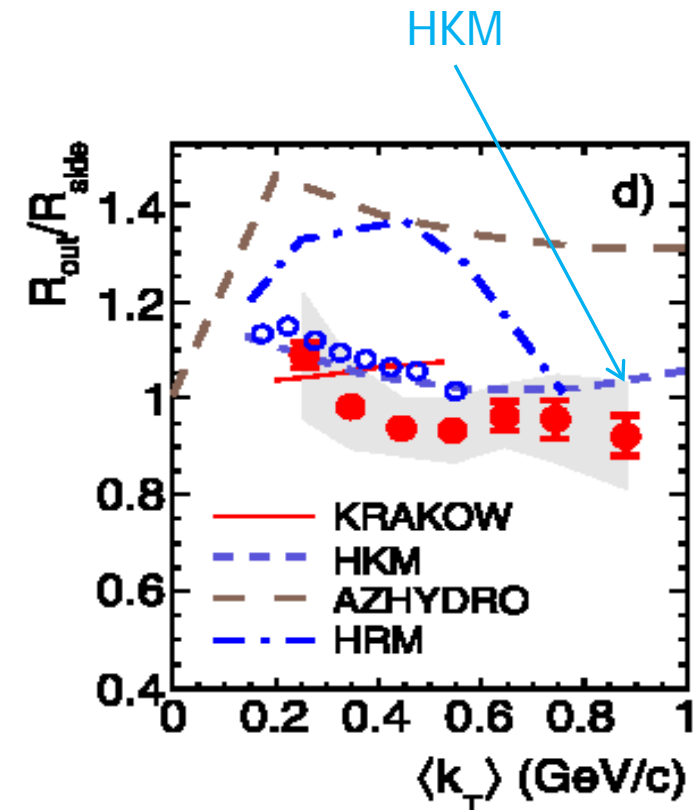
HKM prediction: solution of the HBT Puzzle

Two-pion Bose–Einstein correlations in central Pb–Pb collisions
at $\sqrt{s_{NN}} = 2.76$ TeV[☆] ALICE Collaboration Physics Letters B 696 (2011) 328.



Quotations:

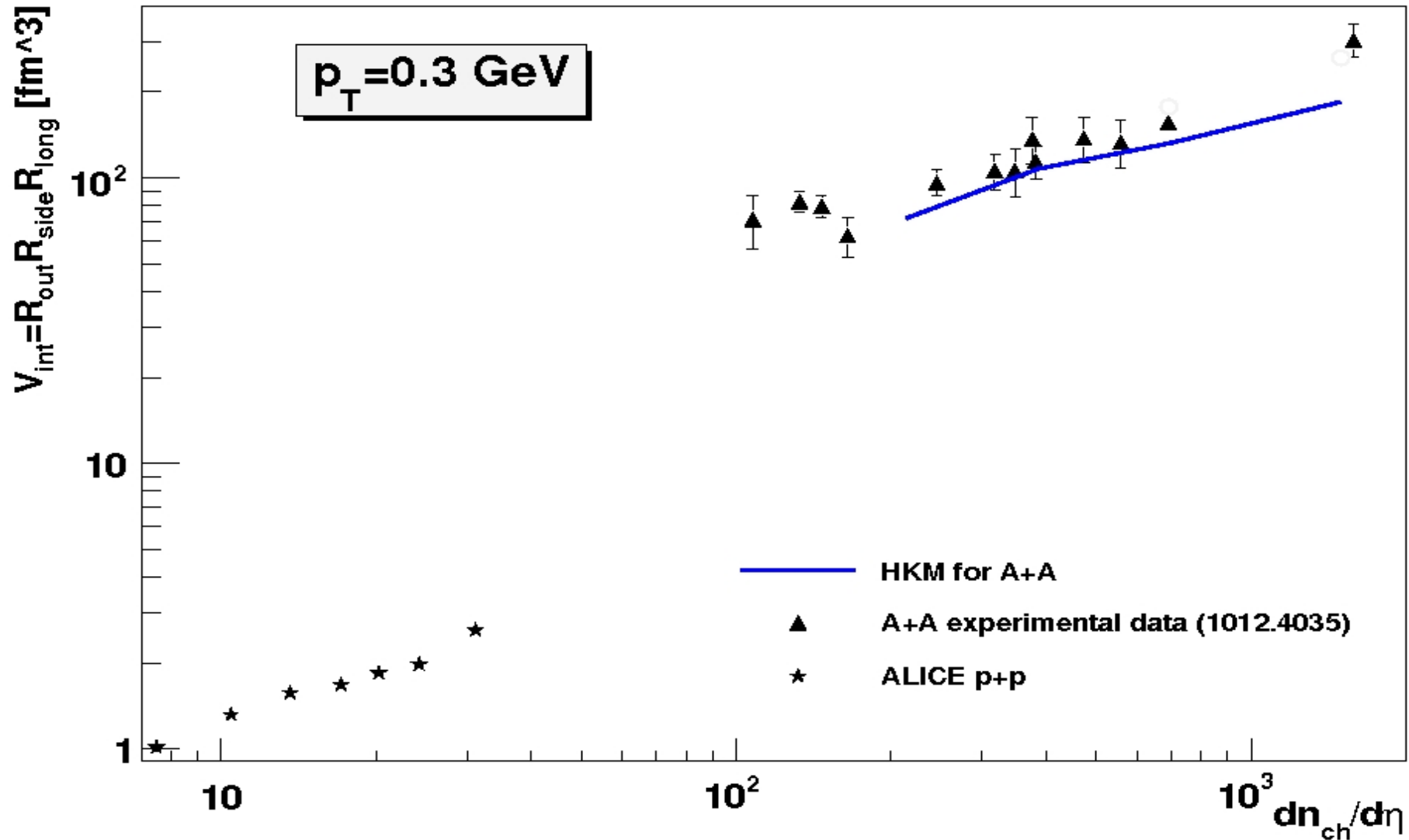
Available model predictions are compared to the experimental data in Figs. 2-d and 3. Calculations from three models incorporating a hydrodynamic approach, AZHYDRO [45], KRAKOW [46,47], and HKM [48,49], and from the hadronic-kinematics-based model HRM [50,51] are shown. An in-depth discussion is beyond the scope of this Letter but we notice that, while the increase of the radii between RHIC and the LHC is roughly reproduced by all four calculations, only two of them (KRAKOW and HKM) are able to describe the experimental R_{out}/R_{side} ratio.



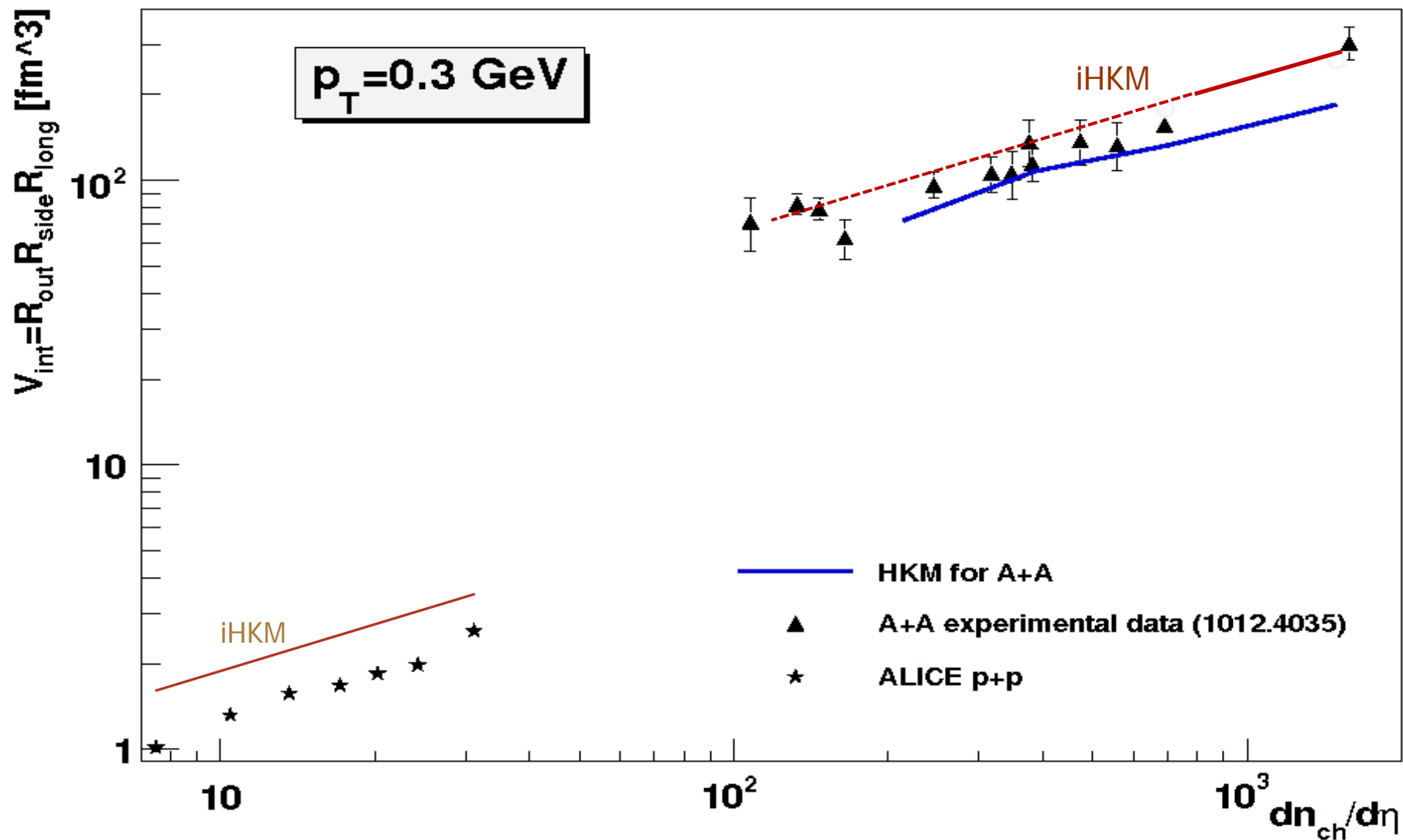
[48] I.A. Karpenko, Y.M. Sinyukov, Phys. Lett. B 688 (2010) 50.

[49] N. Armesto, et al. (Eds.), J. Phys. G 35 (2008) 054001.

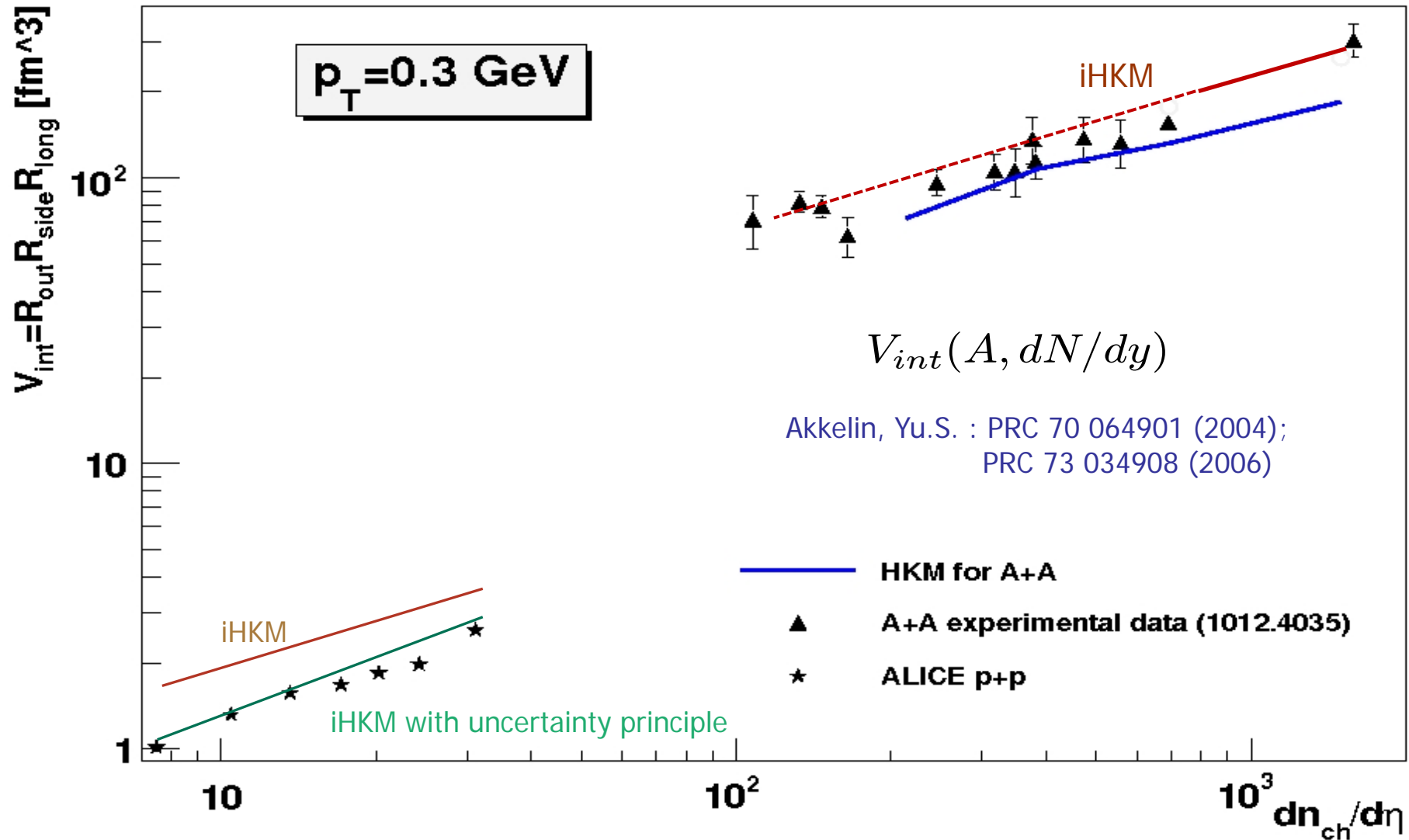
Interferometry volume V_{int} in LHC p-p and **central** Au-Au, Pb-Pb collisions



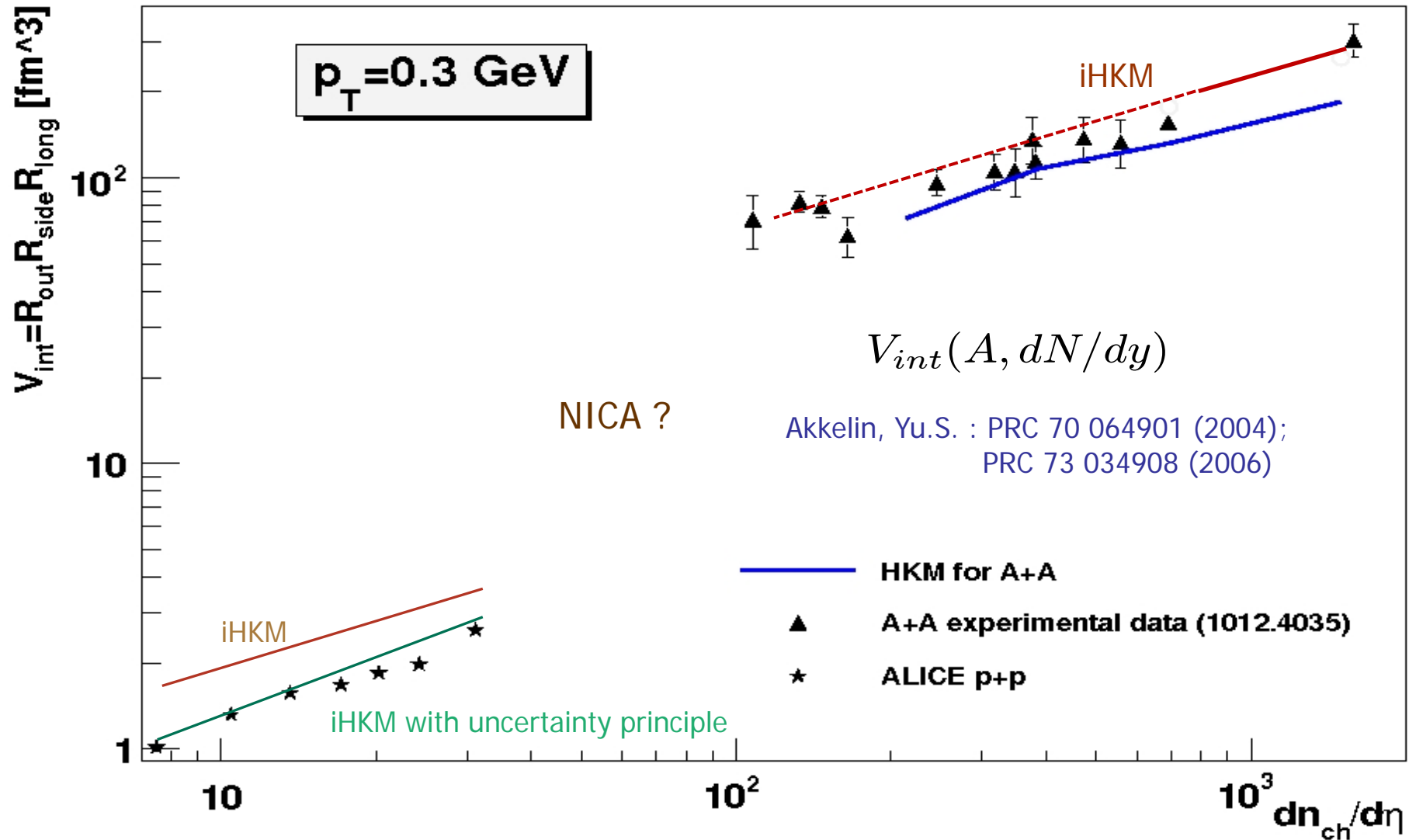
Interferometry volume V_{int} in LHC p-p and **central** Au-Au, Pb-Pb collisions

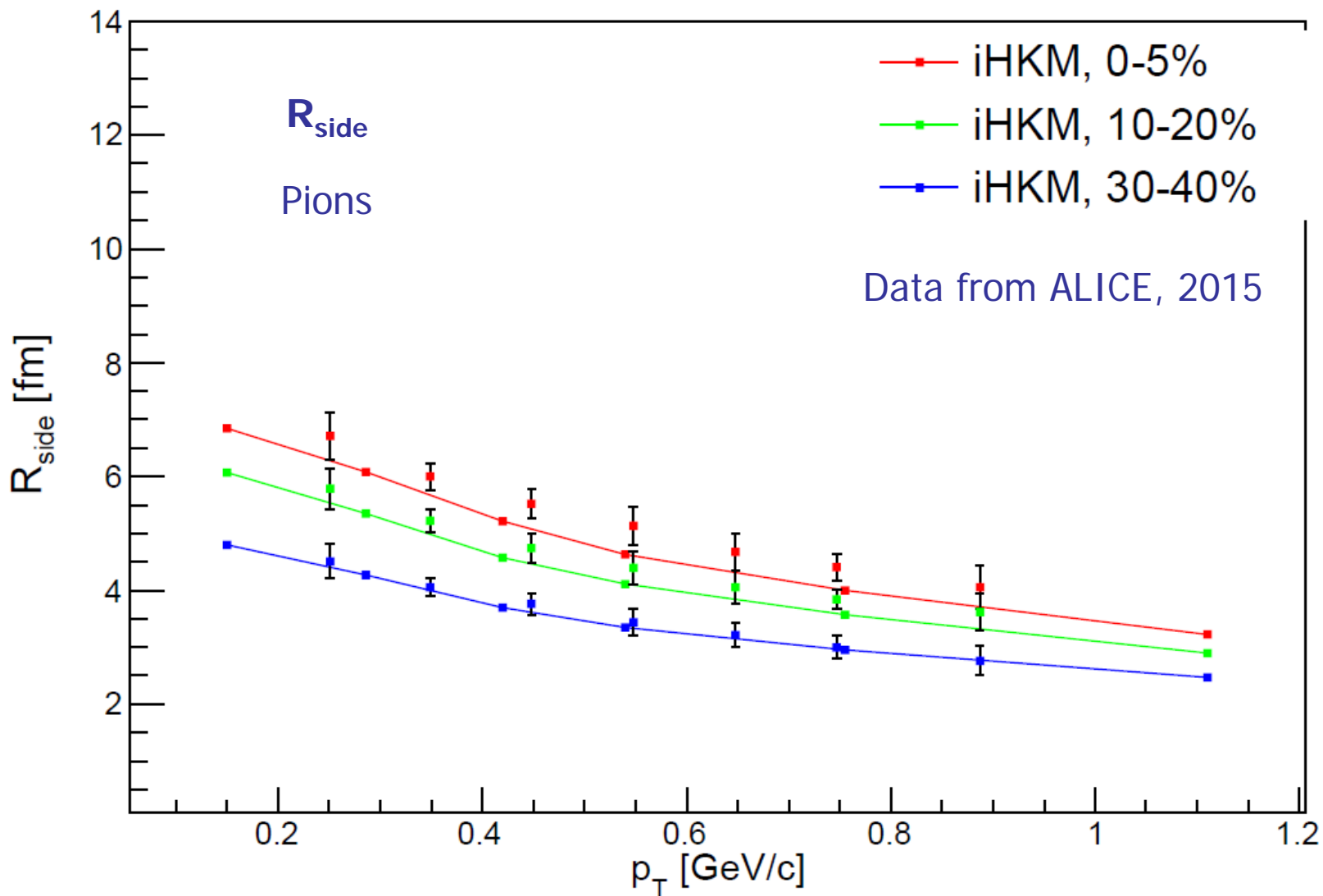


Interferometry volume V_{int} in LHC p-p and **central** Au-Au, Pb-Pb collisions



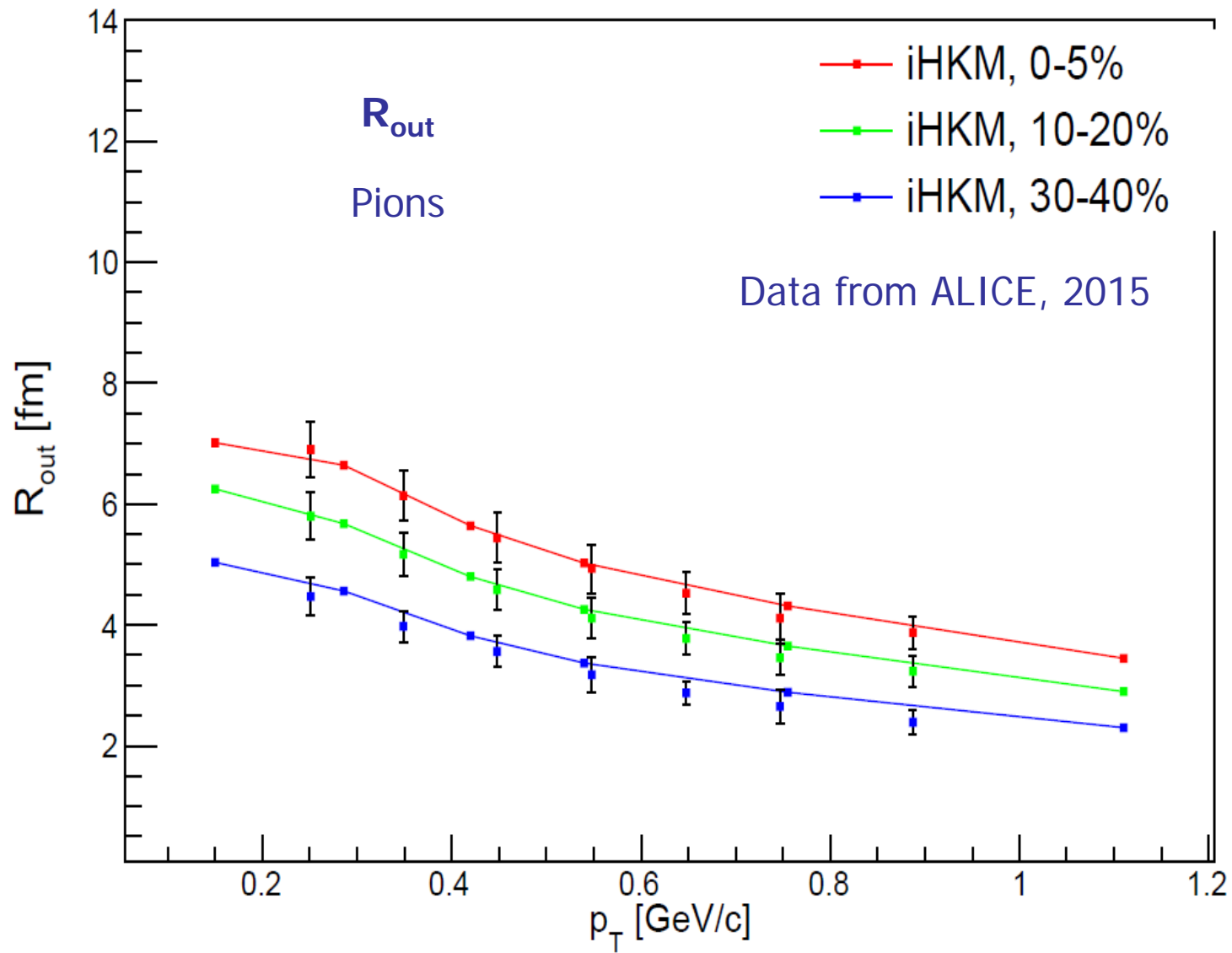
Interferometry volume V_{int} in LHC p-p and **central** Au-Au, Pb-Pb collisions



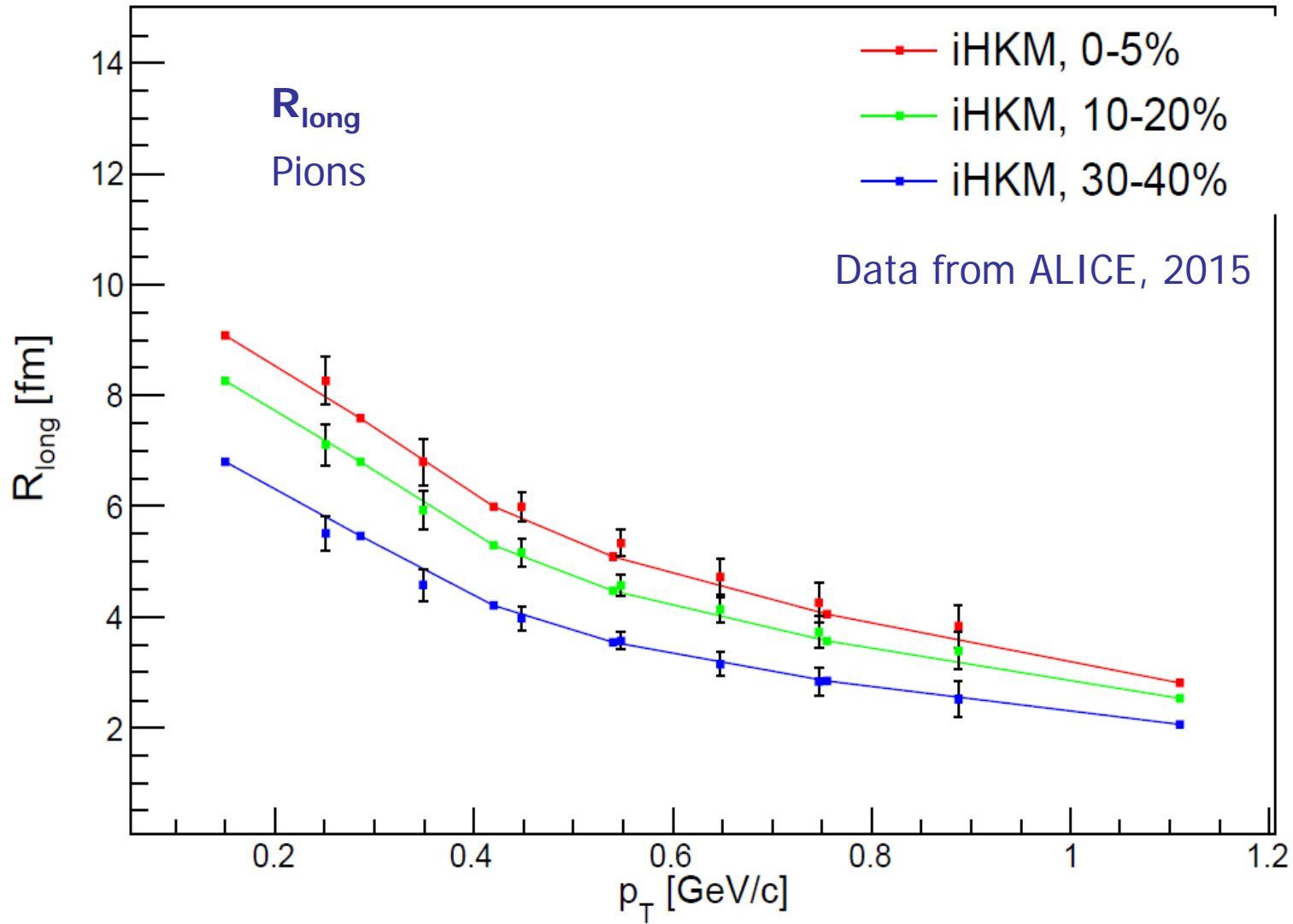


The R_{side} dependence on transverse momentum for different centralities in the iHKM

scenario under the same conditions as in Fig. 1. The experimental data are from [33].



The R_{out} dependence on transverse momentum for different centralities in the iHKM basic scenario under the same conditions as in Fig. 1.



The R_{long} dependence on transverse momentum for different centralities in the iHKM basic scenario - the same conditions as in Fig. 1. The experimental data are from [33].

STAR Collaboration

arXiv:1302.3168 February 2013

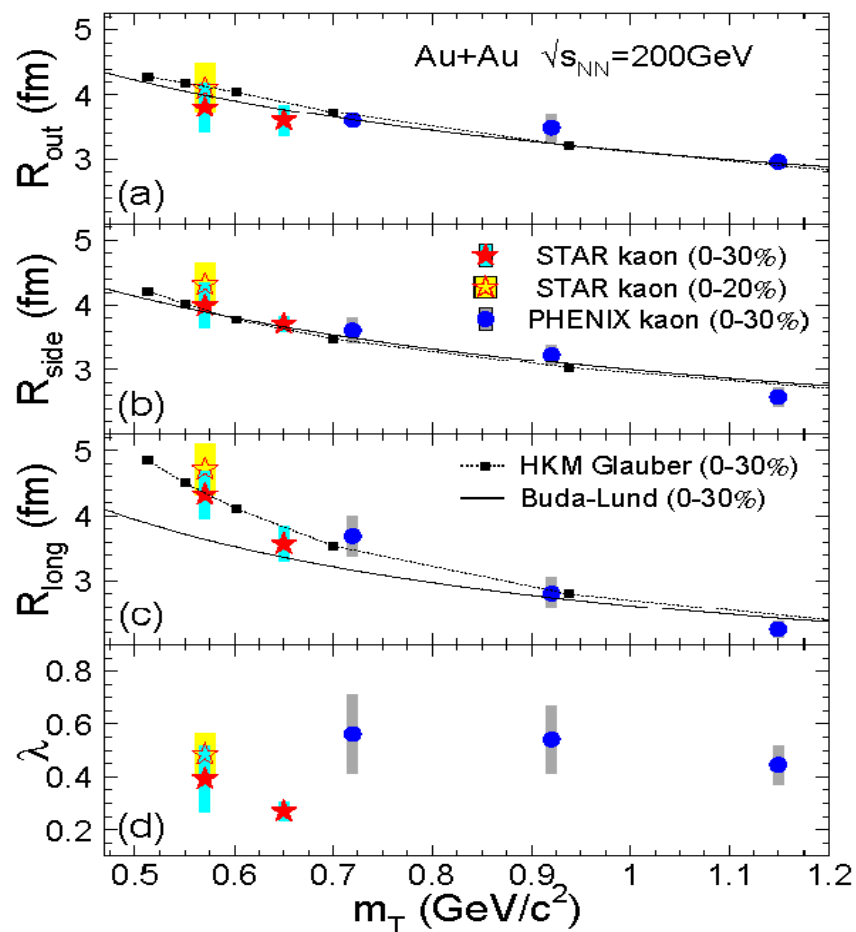


FIG. 4. Transverse mass dependence of Gaussian radii (a) R_{out} , (b) R_{side} and (c) R_{long} for mid-rapidity kaon pairs from the 30% most central Au+Au collisions at $\sqrt{s_{NN}}=200$ GeV. STAR data are shown as solid stars; PHENIX data [10] as solid circles (error bars include both statistical and systematic uncertainties). Hydro-kinetic model [23] with initial Glauber condition and Buda-Lund model [22] calculations are shown by solid squares and solid curves, respectively.

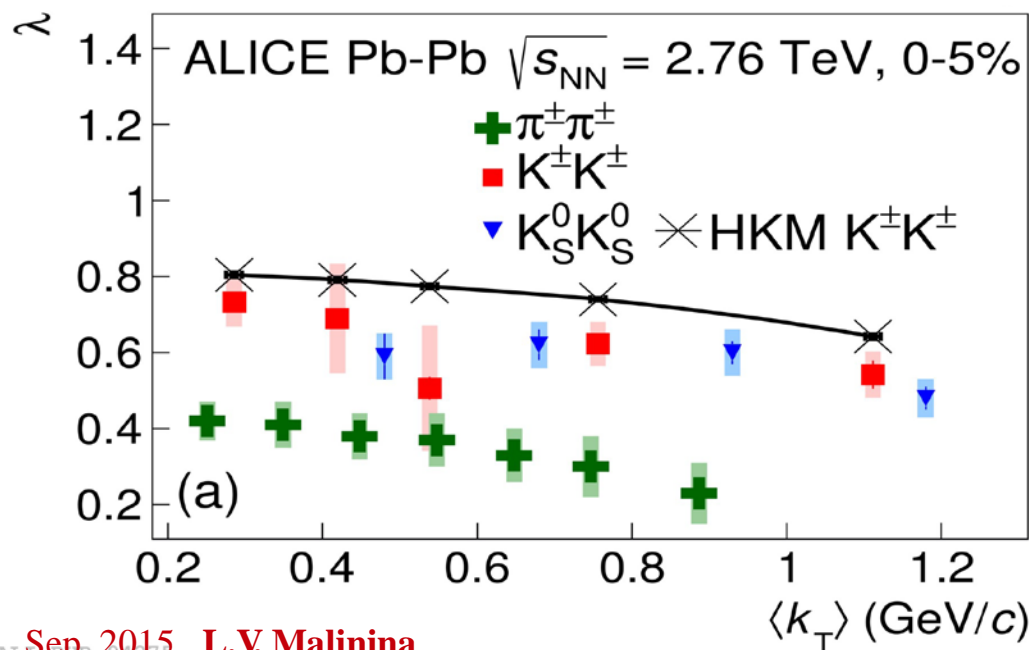
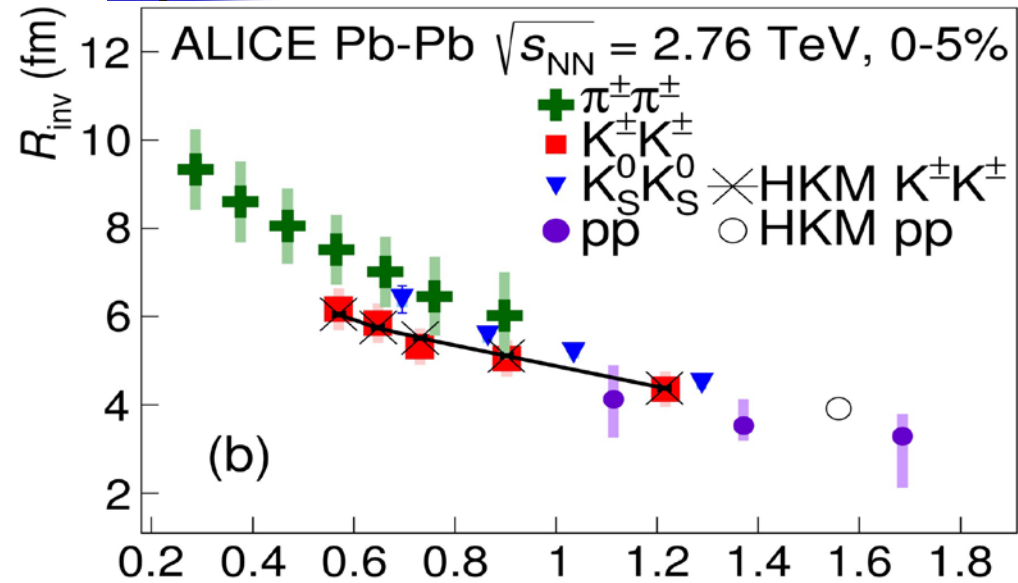
Quotations:

Our measurement at $0.2 \leq k_T \leq 0.36$ GeV/c clearly favours the HKM model as more representative of the expansion dynamics of the fireball.

In the outward and side-ward directions, this decrease is adequately described by m_T -scaling. However, in the longitudinal direction, the scaling is broken. The results are in favor of the hydro-kinetic predictions [23] over pure hydrodynamical model calculations.

[23] I. A. Karpenko and Y. M. Sinyukov, Phys. Rev. C **81** (2010) 054903.

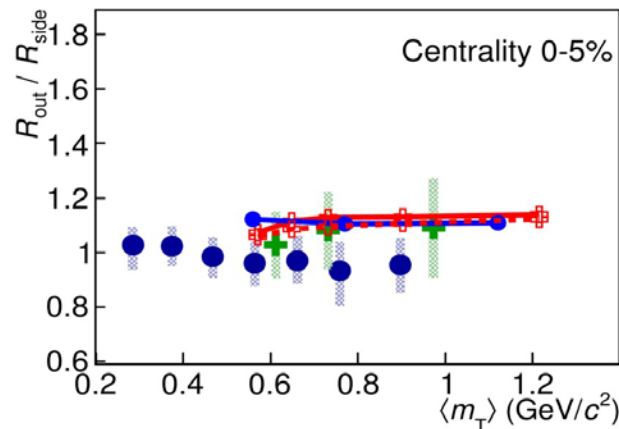
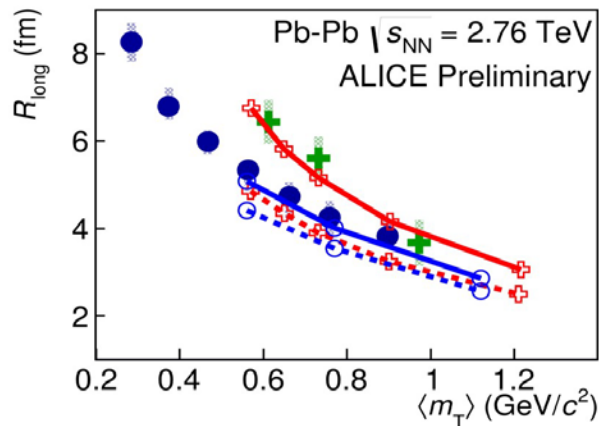
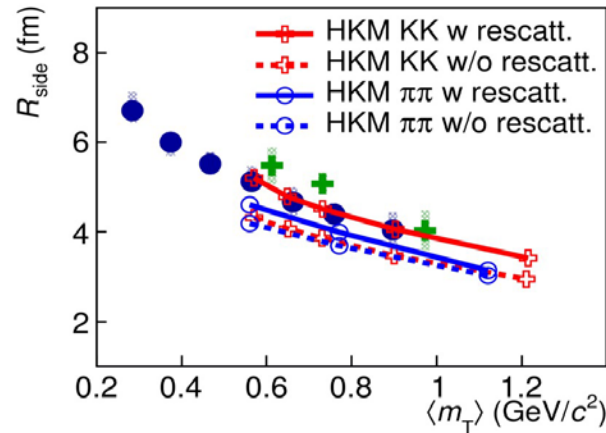
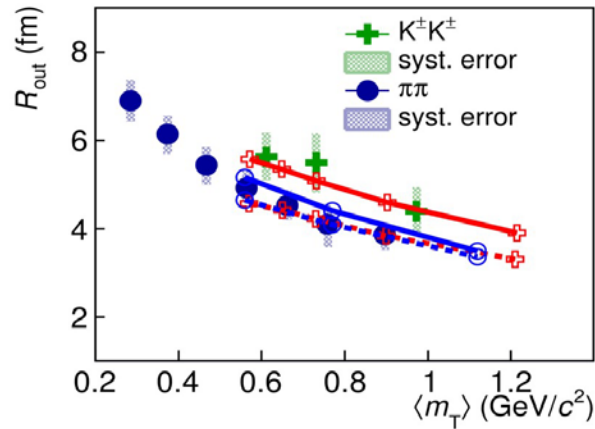
1D $K^\pm K^\pm$ and $K^0_S K^0_S$ in Pb-Pb: HKM model



New results from [ArXiv.org:1506.07884](https://arxiv.org/abs/1506.07884)

- R and λ for $\pi^\pm \pi^\pm$, $K^\pm K^\pm$, $K^0_S K^0_S$, pp for 0-5% centrality
- Radii for kaons show good agreement with **HKM predictions** for $K^\pm K^\pm$
(V. Shapoval, P. Braun-Munzinger, Yu. Sinyukov Nucl.Phys.A929 (2014))
- λ decrease with k_T , both data and HKM
- HKM prediction for λ slightly overpredicts the data
- Λ_π are lower λ_K due to the stronger influence of resonances

Comparison with HKM for 0-5% centrality



- HKM model with re-scatterings (M. Shapoval, P. Braun-Munzinger, Iu.A. Karpenko, Yu.M. Sinyukov, Nucl.Phys. A 929 (2014) 1.) describes well ALICE π & K data.

● HKM model w/o re-scatterings demonstrates

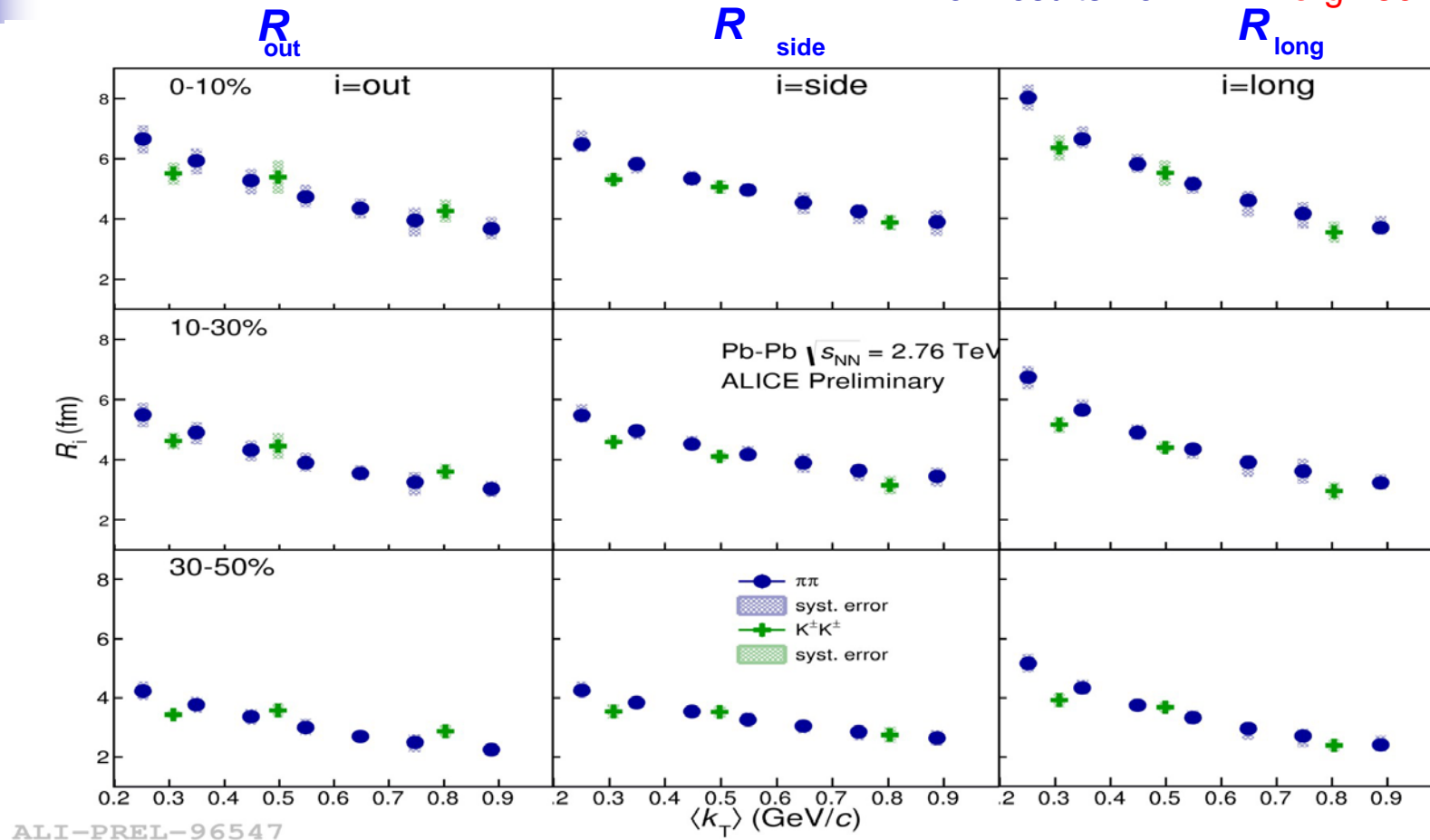
approximate m_T scaling for π & K, but does not describe ALICE π & K data

- The observed deviation from m_T scaling is explained in (M. Shapoval, P. Braun-Munzinger, Iu.A. Karpenko, Yu.M. Sinyukov, Nucl.Phys. A 929 (2014) by essential transverse flow & re-scattering phase.

● HKM model slightly underestimates R_{side}

3D $K^\pm K^\pm$ & $\pi\pi$ radii versus k_T

Pion results from [ArXiv.org:1507.06842](https://arxiv.org/abs/1507.06842)

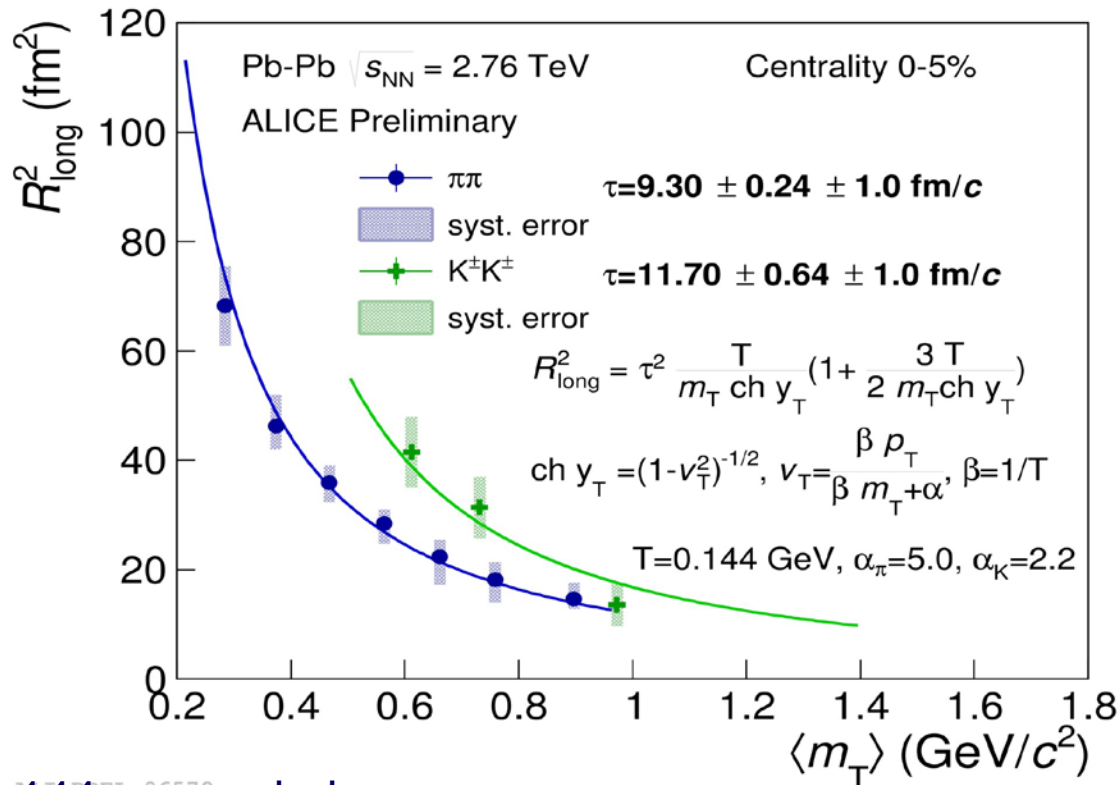
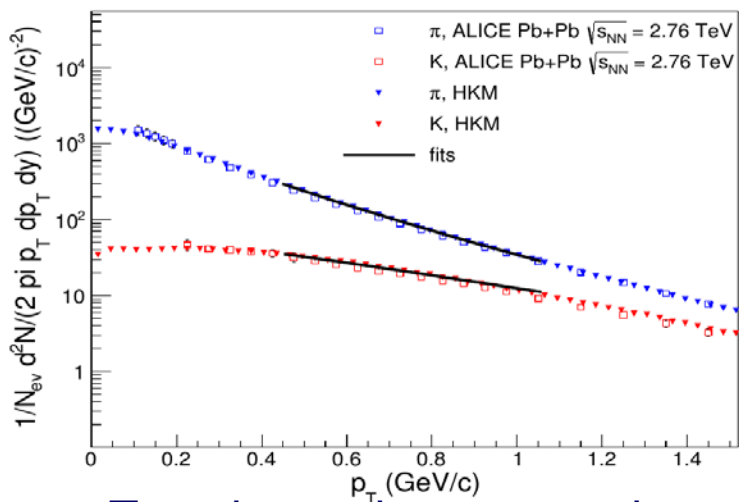


- Radii scale better with k_T than with m_T according with HKM predictions
(V. Shapoval, P. Braun-Munzinger, Iu.A. Karpenko, Yu.M. Sinyukov, Nucl.Phys. A 929 (2014) 1);
- Similar observations were reported by PHENIX at RHIC ([arxiv:1504.05168](https://arxiv.org/abs/1504.05168)).

Extraction of emission time from fit R_{long}

The new formula for extraction of the maximal emission time for the case of strong transverse flow was used (Yu. S., Shapoval, Naboka, Nucl. Phys. A 946 (2016) 227)

The parameters of freeze-out: T and “intensity of transverse flow” α were fixed by fitting π and K spectra (arxiv:1508.01812)



To estimate the systematic errors: $T = 0.144$ was varied on ± 0.03 GeV & free α_{π}, α_K were used; systematic errors ~ 1 fm/c

Indication: $\tau_{\pi} < \tau_K$. Possible explanations (arxiv:1508.01812): HKM includes re-scatterings (UrQMD cascade): e.g. $K\pi \rightarrow K^*(892) \rightarrow K\pi$, $KN \rightarrow K^*(892)X$; ($K^*(892)$ lifetime 4-5 fm/c) [$\pi N \rightarrow N^*(\Delta)X$, $N^*(\Delta) \rightarrow \pi X$ (N^* 's(Δ s)- short lifetime)]

Space-time picture of the pion and kaon emission

$$R_l^2(k_T) = \underbrace{\tau^2 \lambda^2 \left(1 + \frac{3}{2} \lambda^2\right)}_{2015} \approx \text{w/o transv. expansion} \approx \underbrace{\tau^2 \frac{T}{m_T}}_{1987} \underbrace{\frac{K_2\left(\frac{m_T}{T}\right)}{K_1\left(\frac{m_T}{T}\right)}}_{1995}$$

where

$$\lambda^2 = \frac{T}{m_T} \left(1 - \frac{\overbrace{k_T^2}^{\bar{v}_T^2}}{(m_T + \alpha T)^2}\right)^{1/2}$$

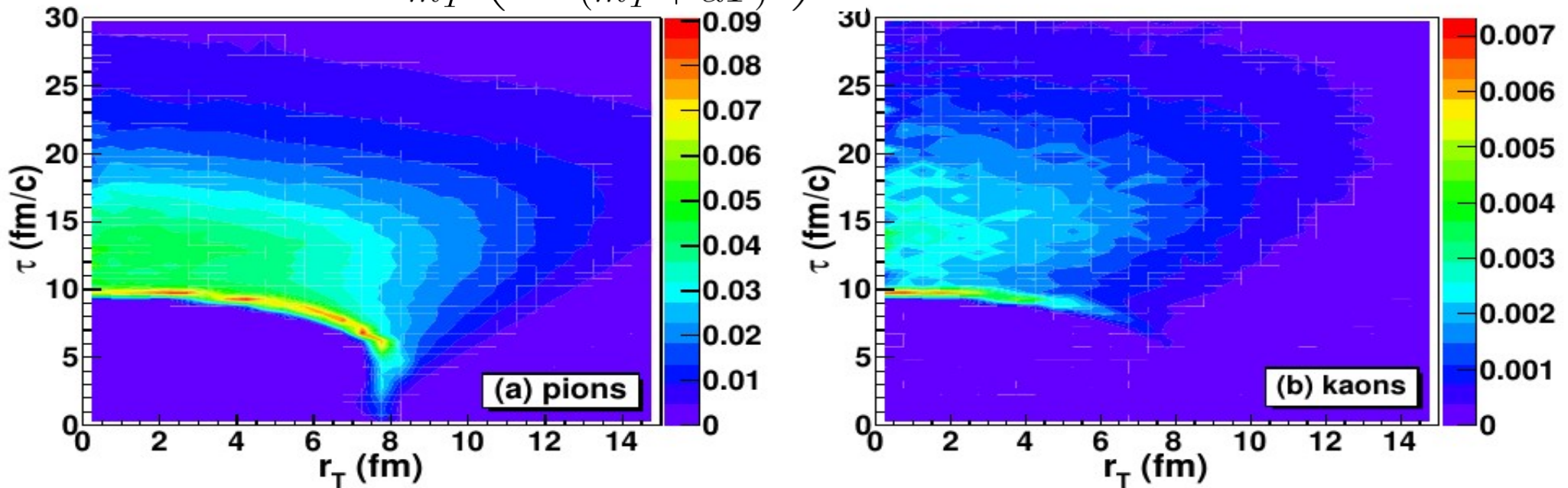


FIG. 4. The momentum angle averaged emission functions per units of space-time and momentum rapidities $g(\tau, r_T, p_T)$ [fm^{-3}] (see body text) for pions (a) and kaons (b) obtained from the HKM simulations of Pb+Pb collisions at the LHC $\sqrt{s_{NN}} = 2.76$ GeV, $0.2 < p_T < 0.3$ GeV/c, $|y| < 0.5$, $e = 0 - 5\%$. From Yu.S., Shapoval, Naboka, Nucl. Phys. A 946 (2016) 247 ([arXiv:1508.01812](https://arxiv.org/abs/1508.01812))

Thermal and evolutionary approaches

Continuous freeze-out vs sudden freeze-out

- Thermal models of particle production vs dynamic/evolutionary approaches

Kinetic/thermal freeze-out

Sudden freeze-out

Cooper-Frye prescription

$$p^0 \frac{d^3 N_i}{d^3 p} = \int_{\sigma_{th}} d\sigma_\mu p^\mu f_i(x, p)$$

The σ_{th} is typically isotherm.

Continuous freeze-out

$$p^0 \frac{d^3 N_i}{d^3 p} = \int d^4 x S_i(x, p) \approx \int_{\sigma(p)} d\sigma_\mu p^\mu f_i(x, p)$$

The $\sigma(p)$ is piece of hypersurface where the particles with momentum near p has a maximal emission rate.
Yu.S. Phys. Rev. C78,

Continuous freeze-out vs sudden freeze-out

- Thermal models of particle production vs dynamic/evolutionary approaches

Kinetic/thermal freeze-out

Sudden freeze-out

Cooper-Frye prescription

$$p^0 \frac{d^3 N_i}{d^3 p} = \int_{\sigma_{th}} d\sigma_\mu p^\mu f_i(x, p)$$

The σ_{th} is typically isotherm.

Continuous freeze-out

$$p^0 \frac{d^3 N_i}{d^3 p} = \int d^4 x S_i(x, p) \approx \int_{\sigma(p)} d\sigma_\mu p^\mu f_i(x, p)$$

The $\sigma(p)$ is piece of hypersurface where the particles with momentum near p has a maximal emission rate.
Yu.S. Phys. Rev. C78,

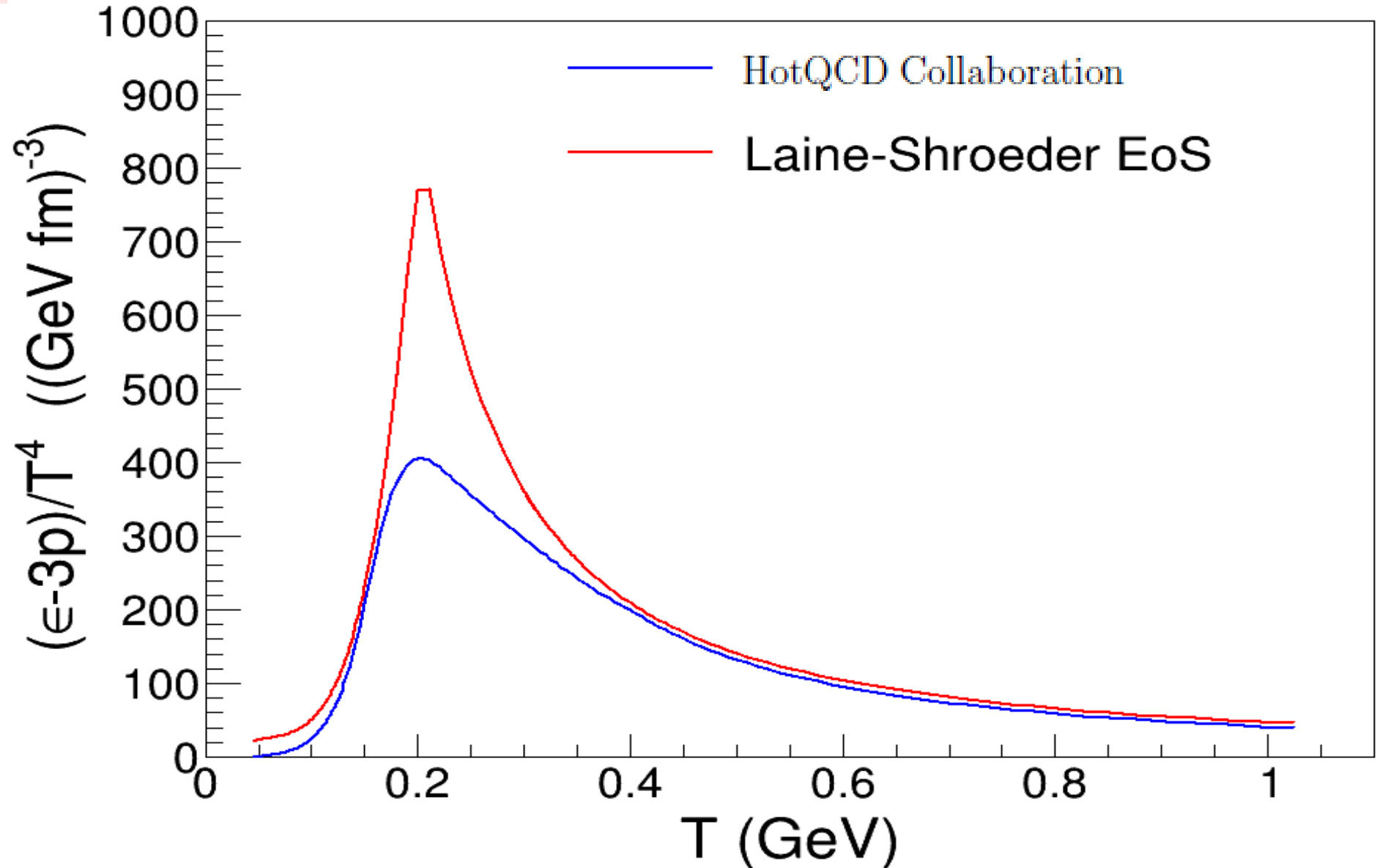
Chemical freeze-out

$$N_i = \int_p \int_{\sigma_{ch}} \frac{d^3 p}{p^0} d\sigma_\mu p^\mu f_i\left(\frac{p^\mu u_\mu(x)}{T_{ch}}, \frac{\mu_{i,ch}}{T_{ch}}\right)$$
$$= n_i(T, \mu) V_{eff} \quad V_{eff} = \int_{\sigma_{ch}} u^\mu d\sigma_\mu$$

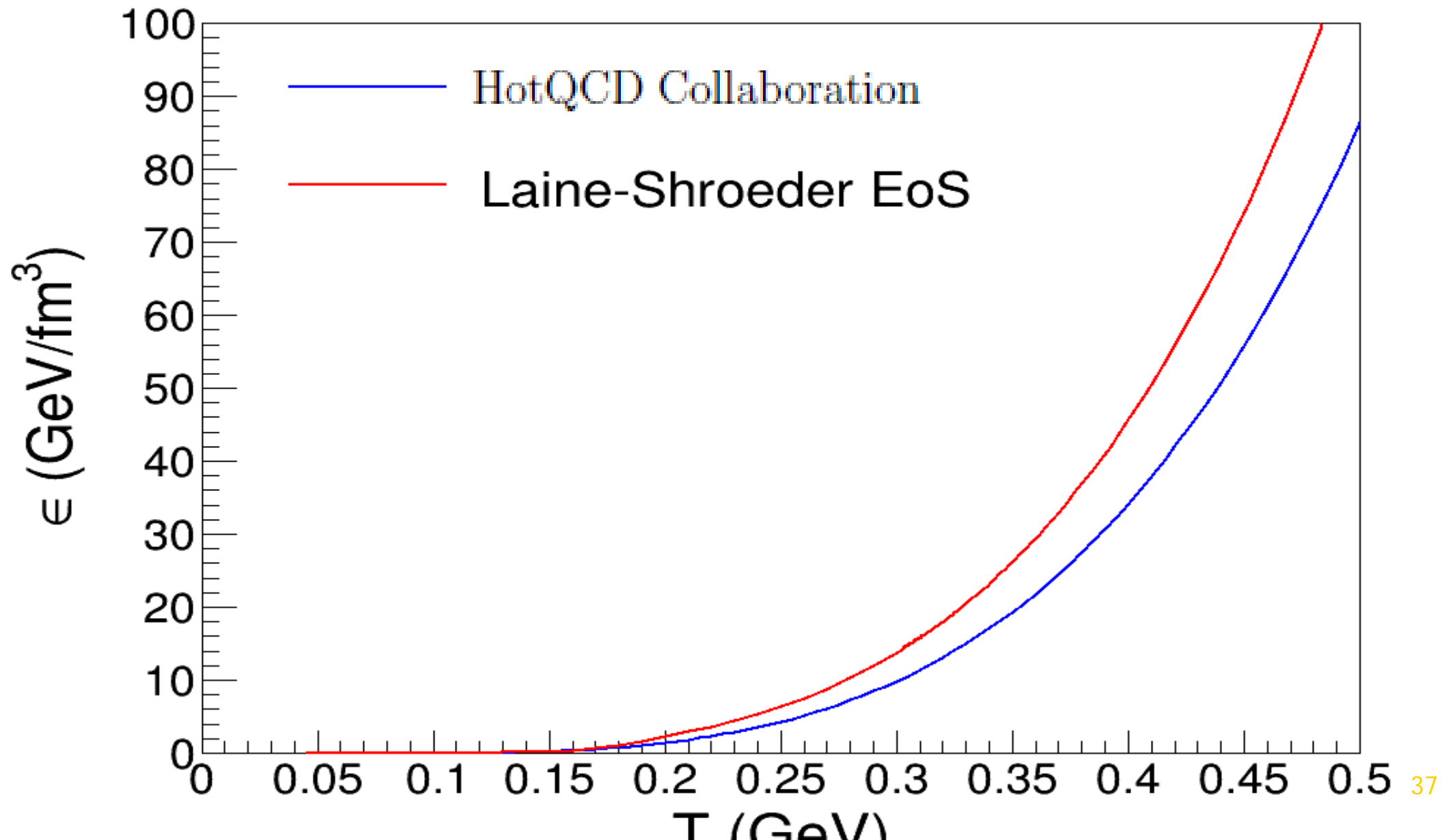
The numbers of quasi-stable particles is defined from N_i with taking into account the resonance decays but **not** inelastic re-scattering.

The T_{ch} is the minimal temperature when the expanding system is still (near) in local thermal and chemical equilibrium. Below the hadronic cascade takes place: $T_{ch} \rightarrow T_{part}$. The inelastic reactions, annihilation processes in hadron-resonance gas change the quasi-particle yields in comparison with sudden chem. freeze-out.

Equation of State - 1



Equation of state -2



Thermal models vs evolutionary approach

Basic matter properties:
thermodynamic **EoS**

Thermal models

Chemical freeze-out at

$$T_{ch} \approx T_h$$

Particle number ratios

$$\left\{ \frac{N_i}{N_j} \right\}$$

Thermal models vs evolutionary approach

Basic matter properties:
thermodynamic **EoS**

Thermal models

Chemical freeze-out at

$$T_{ch} \approx T_h$$

Particle number ratios

$$\left\{ \frac{N_i}{N_j} \right\}$$

Evolutionary models

$$\frac{dN_{charge}}{d\eta}(c)$$

$$\frac{dN_\pi}{p_T dp_T dy}$$

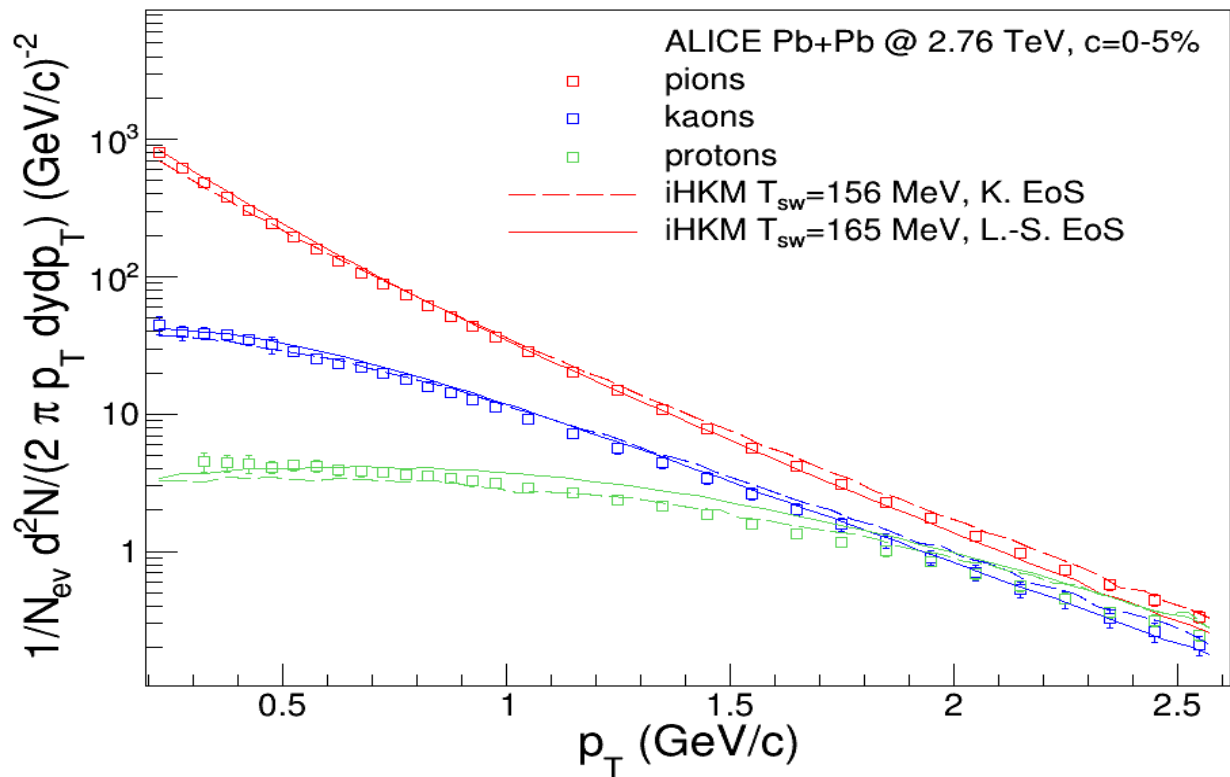
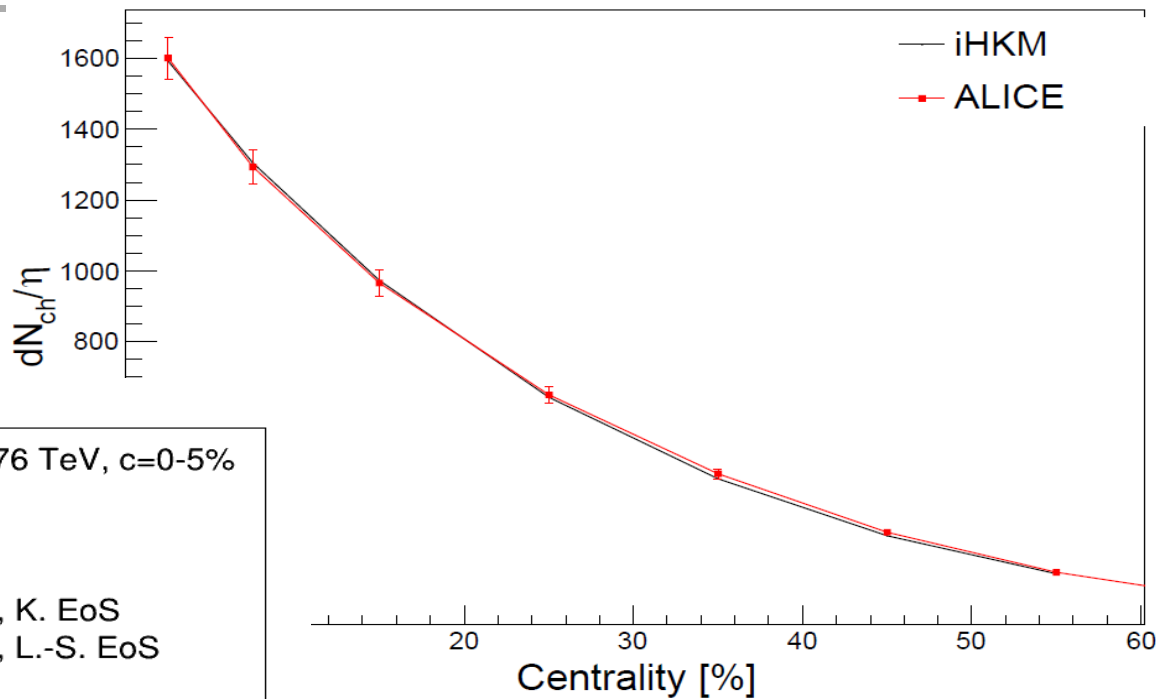
High dense matter formation
time τ_0

Max. energy
density $\epsilon(\tau_0) \equiv \epsilon_0$

EoS defines both particization temperature $T_{part} \approx T_h$ **and** through hydrodynamic evolution the initial collective velocities for post-hydrodynamic evolution of interacting hadron gas where the inelastic reactions including annihilation can happen. It may change particle number ratios. So, to what extend the "chemical freeze-out" is continuous in evolutionary models depends on the rate of expansion at the end of the hydrodynamic stage. In its turn it is defined by the τ_0 and $\epsilon(\tau_0) \equiv \epsilon_0$.

Multiplicity dependence of all charged particles on centrality and spectra for LHC energy

$\sqrt{s_{NN}} = 2.76 \text{ TeV}$



Thermal models vs evolutionary approach

Basic matter properties:
thermodynamic **EoS**

Thermal models

Chemical freeze-out at

$$T_{ch} \approx T_h$$

Particle number ratios

$$\left\{ \frac{N_i}{N_j} \right\}$$

L.-S. \rightarrow Karsch, Fodor (HotQCD)

Evolutionary models

$$\frac{dN_{charge}}{d\eta}(c)$$

$$\frac{dN_\pi}{p_T dp_T}$$

High dense matter formation
time τ_0

Max. energy
density $\epsilon(\tau_0) \equiv \epsilon_0$

At the particlization temperature $T_{part} \approx T_h$
hydrodynamic evolution transforms (suddenly or
continuously) into interact. hadron gas evolution.

EoS:

$$T_h = 165 MeV \rightarrow 156 MeV$$

$$\tau_0 = 0.1 \text{ fm/c} \rightarrow 0.15 \text{ fm/c}$$

$$\epsilon_0 = 679 \text{ GeV/fm}^3 \rightarrow 495 \text{ GeV/fm}^3$$

iHKM

Thermal models vs evolutionary approach

Basic matter properties:
thermodynamic **EoS**

Thermal models

Chemical freeze-out at

$$T_{ch} \approx T_h$$

Particle number ratios

$$\left\{ \frac{N_i}{N_j} \right\}$$

L.-S. \longrightarrow Karsch, Fodor (lattice QCD)

EoS:

$$T_h = 165 \text{ MeV} \longrightarrow 156 \text{ MeV}$$

$$\tau_0 = 0.1 \text{ fm/c} \longrightarrow 0.15 \text{ fm/c}$$

$$\epsilon_0 = 679 \text{ GeV/fm}^3 \longrightarrow 495 \text{ GeV/fm}^3$$

iHKM

Evolutionary models

$$\frac{dN_{charge}}{d\eta}(c)$$

$$\frac{dN_\pi}{p_T dp_T}$$

High dense matter formation time τ_0

Max. energy density $\epsilon(\tau_0) \equiv \epsilon_0$

At the particlization temperature $T_{part} \approx T_h$ hydrodynamic evolution transforms (suddenly or continuously) into interact. hadron gas evolution.

Kinetic freeze-out

«Blast-wave» parametrization of sharp freeze-out hypersurface and transverse flows on it. Spectra $\frac{dN_i}{p_T dp_T} \longrightarrow T_{th}$

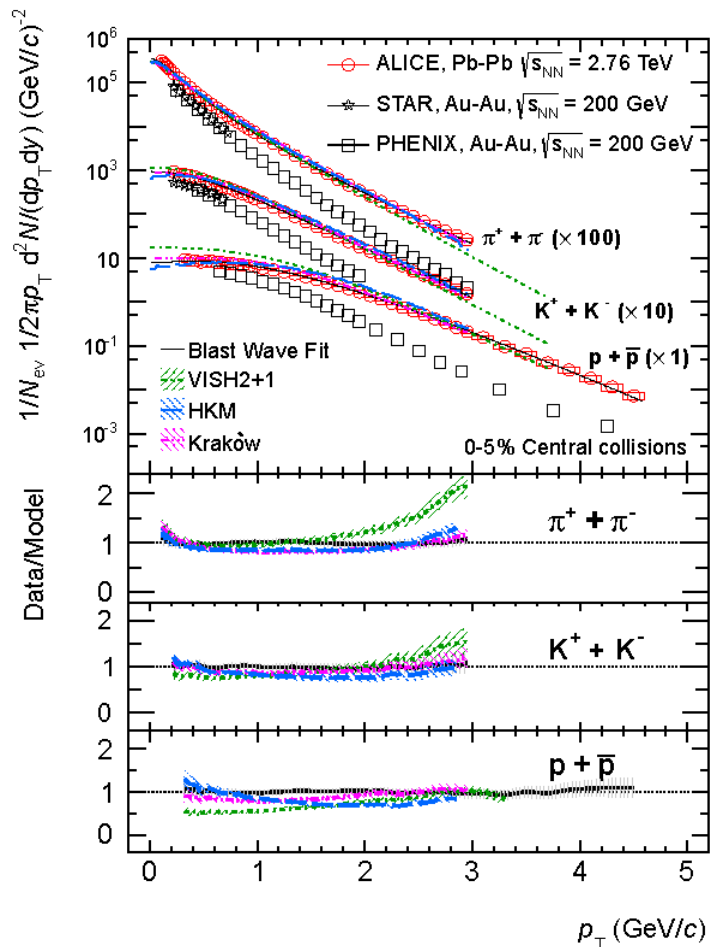
“Effective temperature” of maximal emission: $T_{th}(p)$
Anyway the kinetic freeze-out in evolutionary models is continuous, how can we check it?

Predictions for particle yield at LHC in central collisions from HKM

Pion, Kaon, and Proton Production in Central Pb–Pb Collisions at

$$\sqrt{s_{NN}} = 2.76 \text{ TeV}$$

The ALICE Collaboration *Phys. Rev. Lett.* **109**, 252301 (2012)



Quotations

This interpretation is supported by the comparison with HKM [39, 40], a similar model in which, after the hydrodynamic phase, particles are injected into a hadronic cascade model (UrQMD [41, 42]), which further transports them until final decoupling. The hadronic phase builds additional radial flow, mostly due to elastic interactions, and affects particle ratios due to inelastic interactions. HKM yields a better description of the data. At the LHC, hadronic final state interactions, and in particular antibaryon-baryon annihilation, may therefore be an important ingredient for the description of particle yields [43, 40], contradicting the scenario of negligible abundance-changing processes in the hadronic phase. The third model shown in Fig. 1 (Kraków [44, 45]) introduces non-equilibrium corrections due to viscosity at the transition from the hydrodynamic description to particles, which change the effective T_{ch} , leading to a good agreement with the data. In the region $p_T \lesssim 3 \text{ GeV}/c$ (Kraków) and $p_T \lesssim 1.5 \text{ GeV}/c$ (HKM) the last two models reproduce the experimental data within $\sim 20\%$, supporting a hydrodynamic interpretation of the transverse momentum spectra at the LHC. These models also describe correctly other features of the space-time evolution of the system, as measured by ALICE with charged pion correlations [46].

[39] Y. Karpenko and Y. Sinyukov, *J.Phys.* **G38**, 124059 (2011), nucl-th/1107.3745.

[40] Y. Karpenko, Y. Sinyukov, and K. Werner, (2012), nucl-th/1204.5351.

Predictions for particle spectra at LHC in non-central collisions

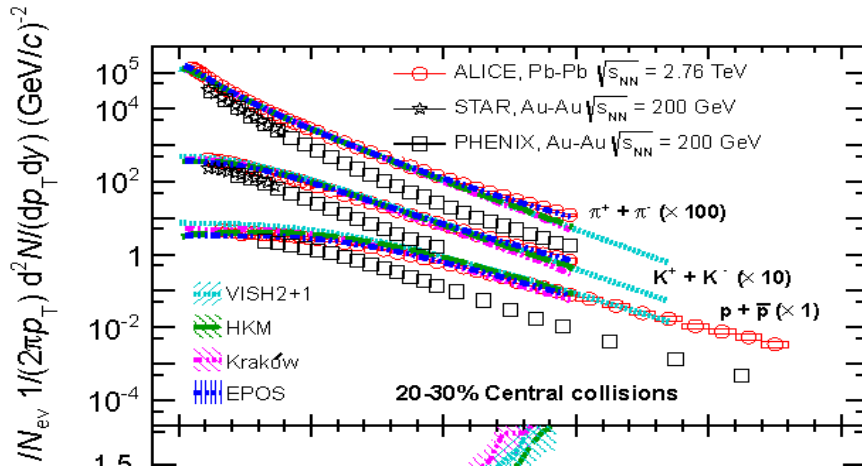
Centrality Dependence of π , K, p in Pb–Pb at $\sqrt{s_{NN}} = 2.76$ TeV

ALICE Collaboration

arXiv:1303.0737v1 [hep-ex]



ALICE



Quotations:

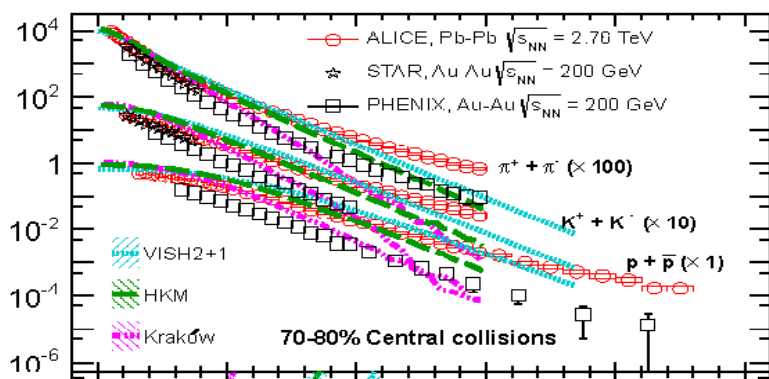
The difference between VISH2+1 and the data are possibly due to the lack of an explicit description of the hadronic phase in the model. This idea is supported by the comparison with HKM [47, 50]. HKM is a model similar to VISH2+1, in which after the hydrodynamic phase particles are injected into a hadronic cascade model (UrQMD), which further transports them until final decoupling. The hadronic phase builds up additional radial flow and affects particle ratios due to the hadronic interactions. As can be seen, this model yields a better description of the data. The protons at low p_T , and hence their total number, are rather well reproduced, even if the slope is significantly smaller than in the data. Antibaryon-baryon annihilation is an important ingredient for the description of particle yields in this model [47, 50].

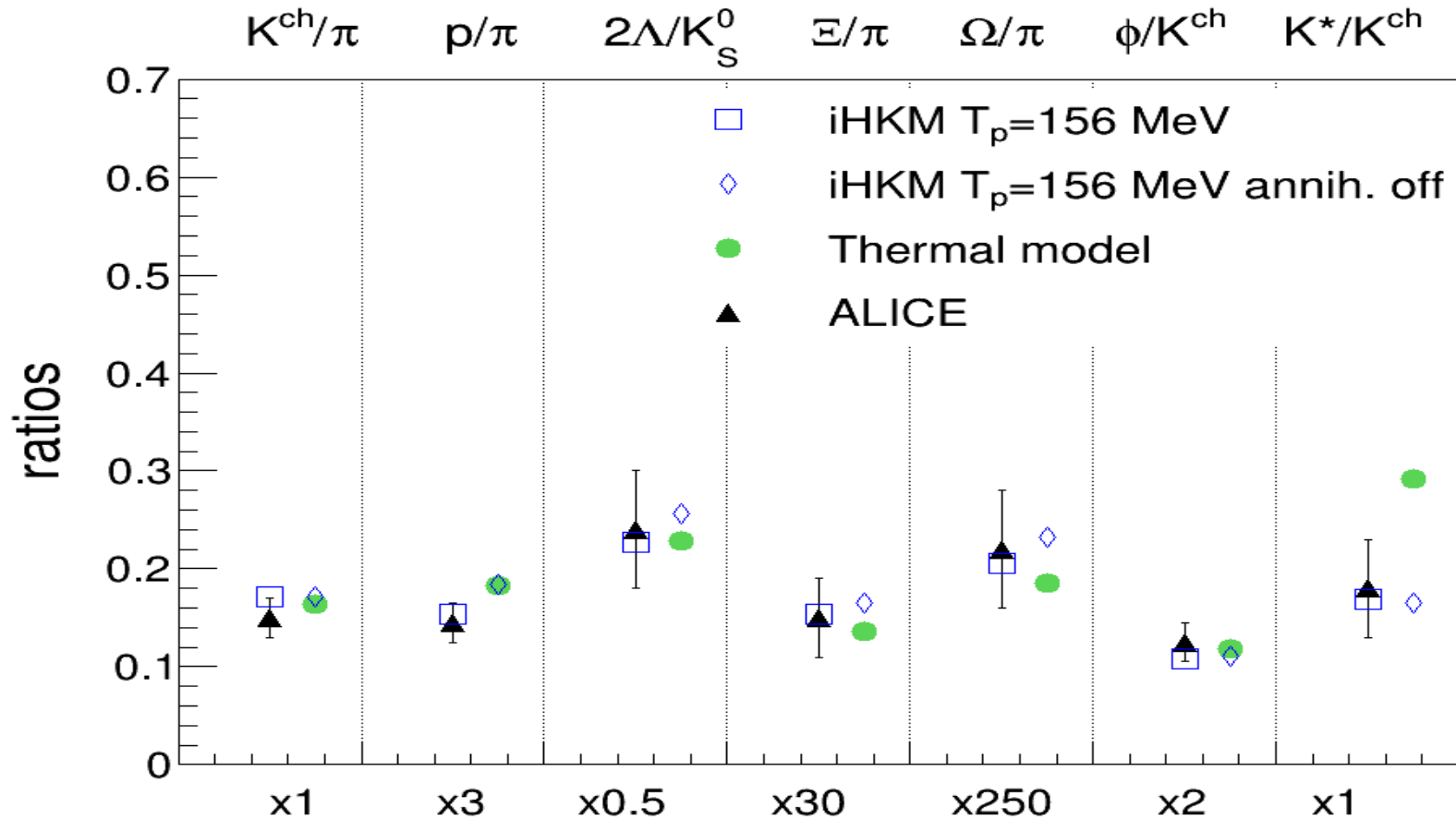
.....

Phys. Rev. C 87, 024914 (2013)

[47] Y. Karpenko, Y. Sinyukov, and K. Werner, (2012), arXiv:1204.5351 [nucl-th]

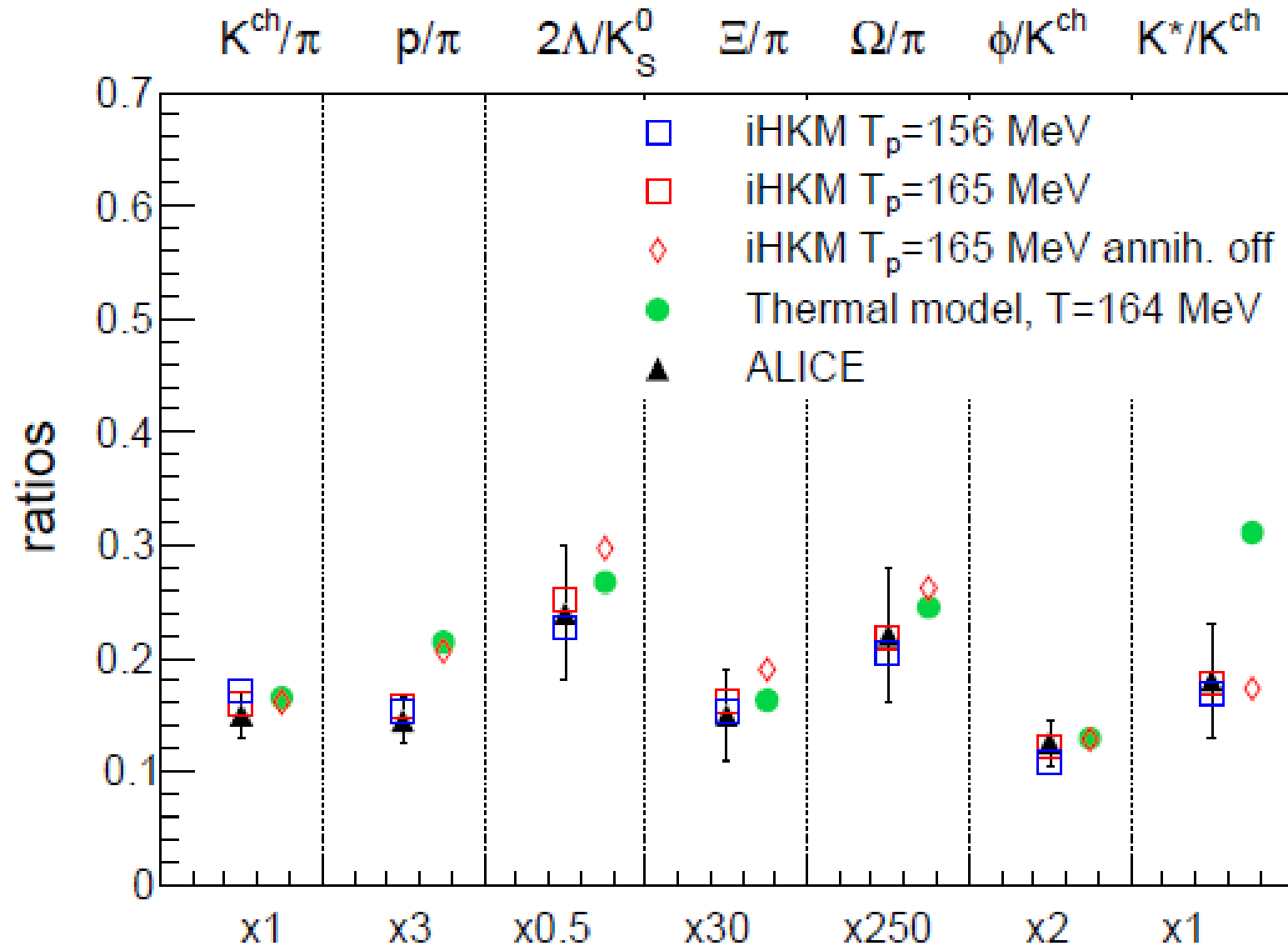
[50] Y. Karpenko and Y. Sinyukov, J.Phys.G **G38**, 124059 (2011).



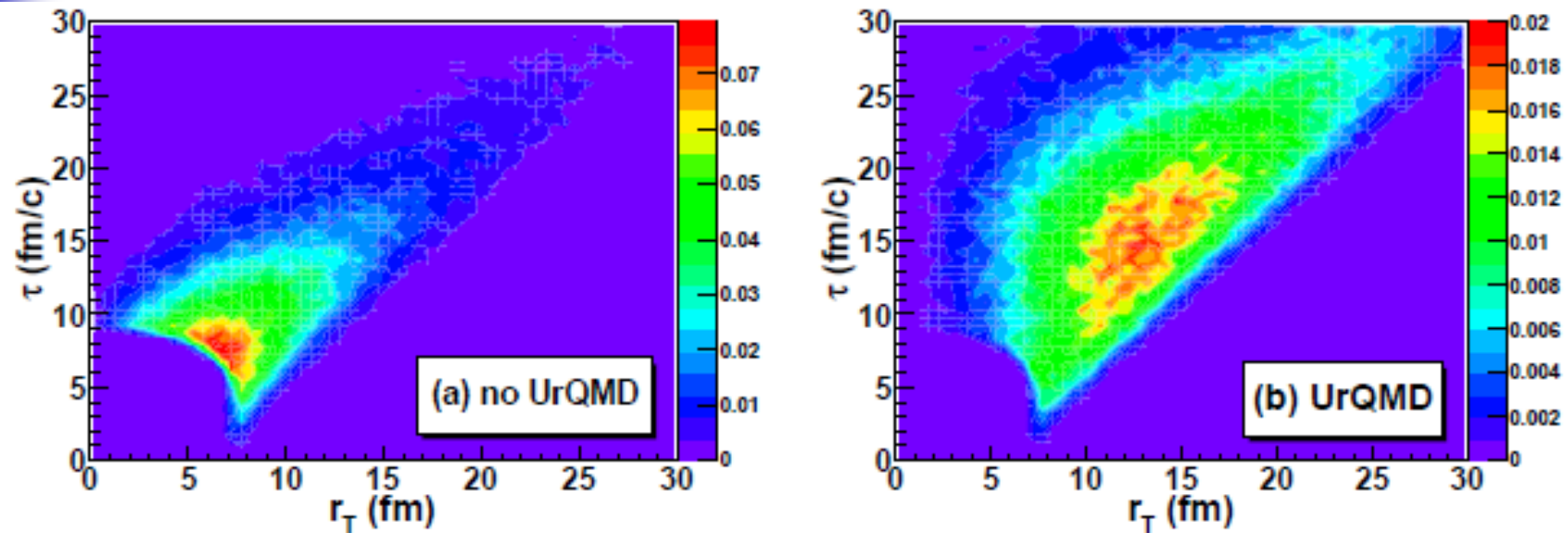


The comparison of particle number ratios, calculated in iHKM (blue and red markers) at the two particlization temperatures and corresponding equations of state with the ALICE experimental data [23] and the thermal model results [24]. The iHKM simulations are performed in two regimes: full calculation and with baryon-antibaryon annihilation switched off.

Particle number ratios at the LHC

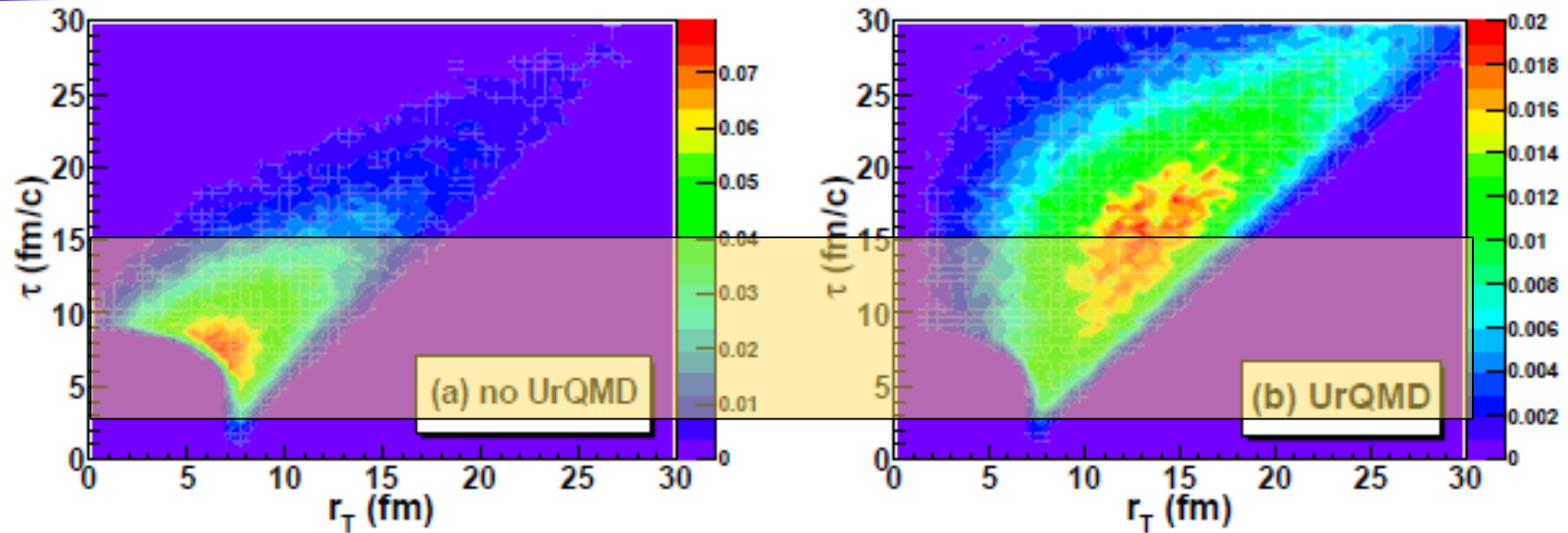


K^* probes



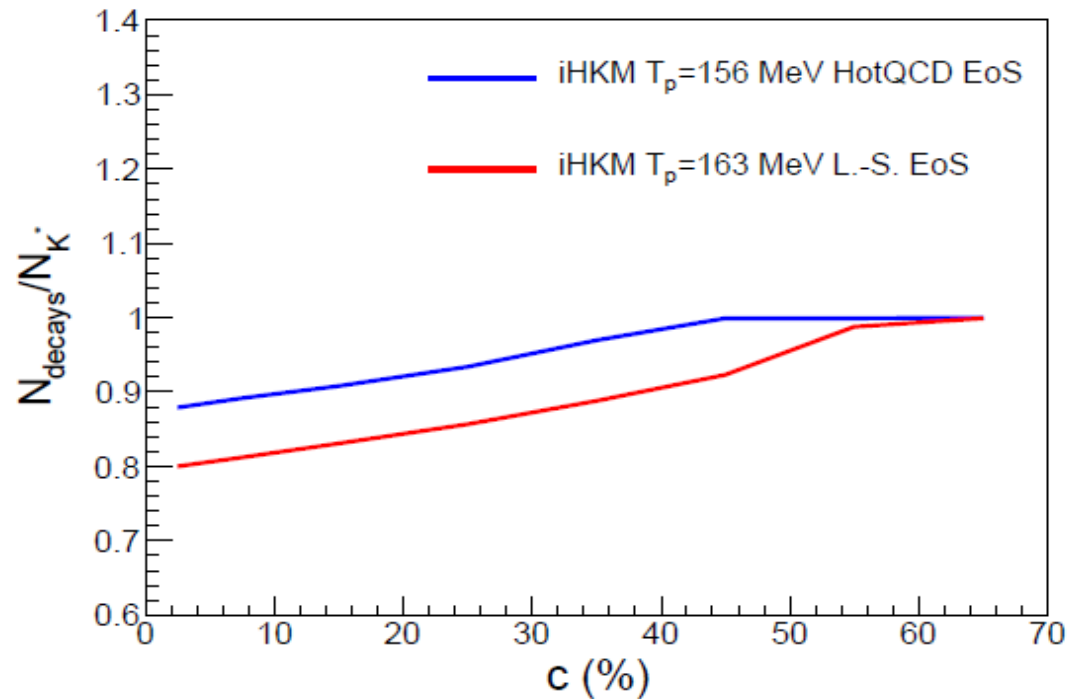
The comparison of the emission functions $g(\tau, r_T)$, averaged over complementary space and momentum components, of $K^+\pi^-$ pairs, associated with $K(892)^{*0}$ decay products, for two cases: (a) free-streaming of the particles and resonances, and (b) UrQMD hadron cascade. The plots are obtained using iHKM simulations of Pb+Pb collisions at the LHC $\sqrt{s_{NN}} = 2.76$ GeV, $0.3 < k_T < 5$ GeV/c, $|y| < 0.5$, $c = 5 - 10\%$.

$K^{*0} \rightarrow K^+\pi^-$ radiation picture in iHKM.
Sudden vs continuous thermal freeze-out at the LHC.



Less than 30% of direct K^* can be seen till 15 fm/c

Suppression of K^{*0} due to continuous thermal freeze-out (LHC)



70% - 20% = 50%
Therefore
at least 50% of direct K^{*0} are
recreated in reactions:

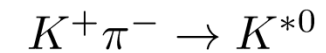
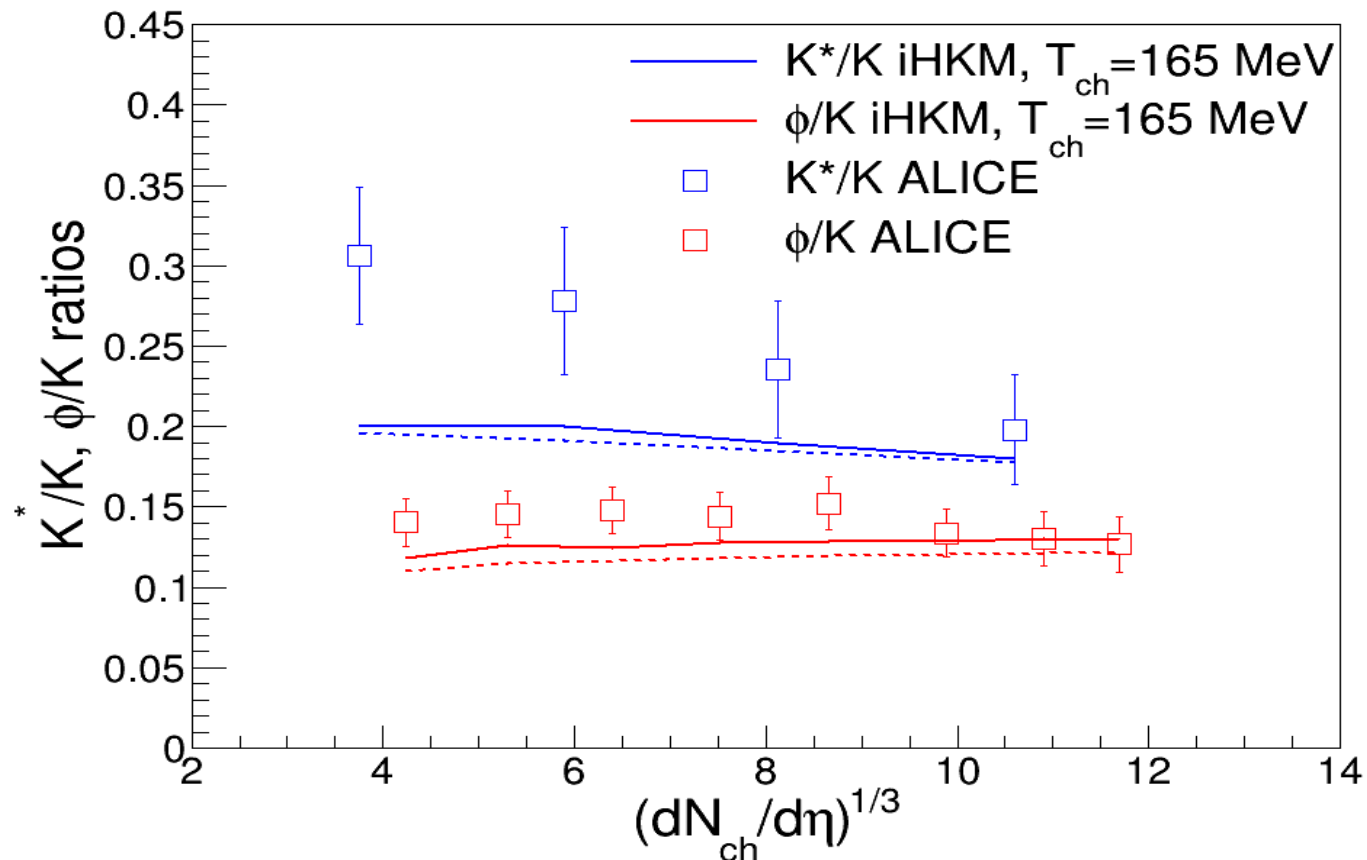


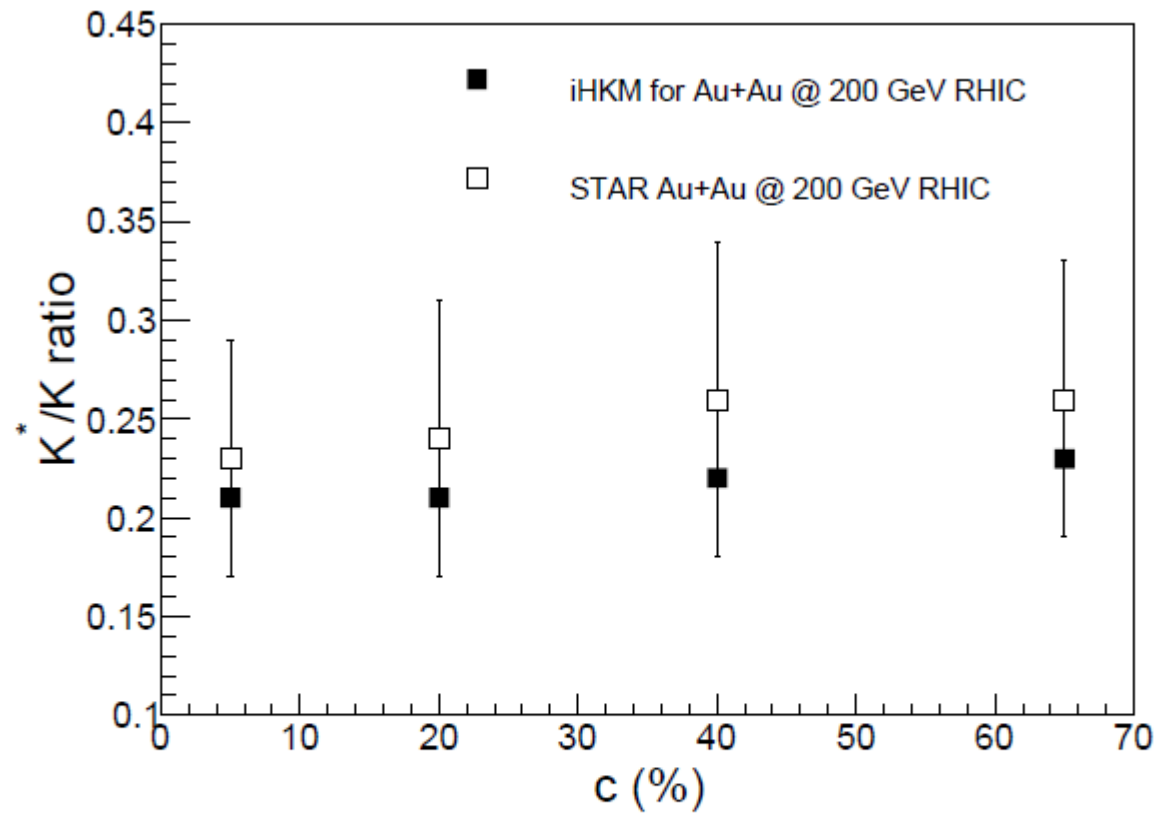
FIG. 3. The fraction of $K^+\pi^-$ pairs coming from $K(892)^*$ decay, which can be identified as daughters of K^* in iHKM simulations after the particle rescattering stage modeled within UrQMD hadron cascade. The simulations correspond to LHC Pb+Pb collisions at $\sqrt{s_{NN}} = 2.76$ TeV with different centralities. The iHKM results are presented for two cases: the Laine-Shroeder equation of state with particlization temperature $T_p = 163$ MeV (red line) and the HotQCD equation of state with $T_p = 156$ MeV (blue line).

Ratios to K (LHC)



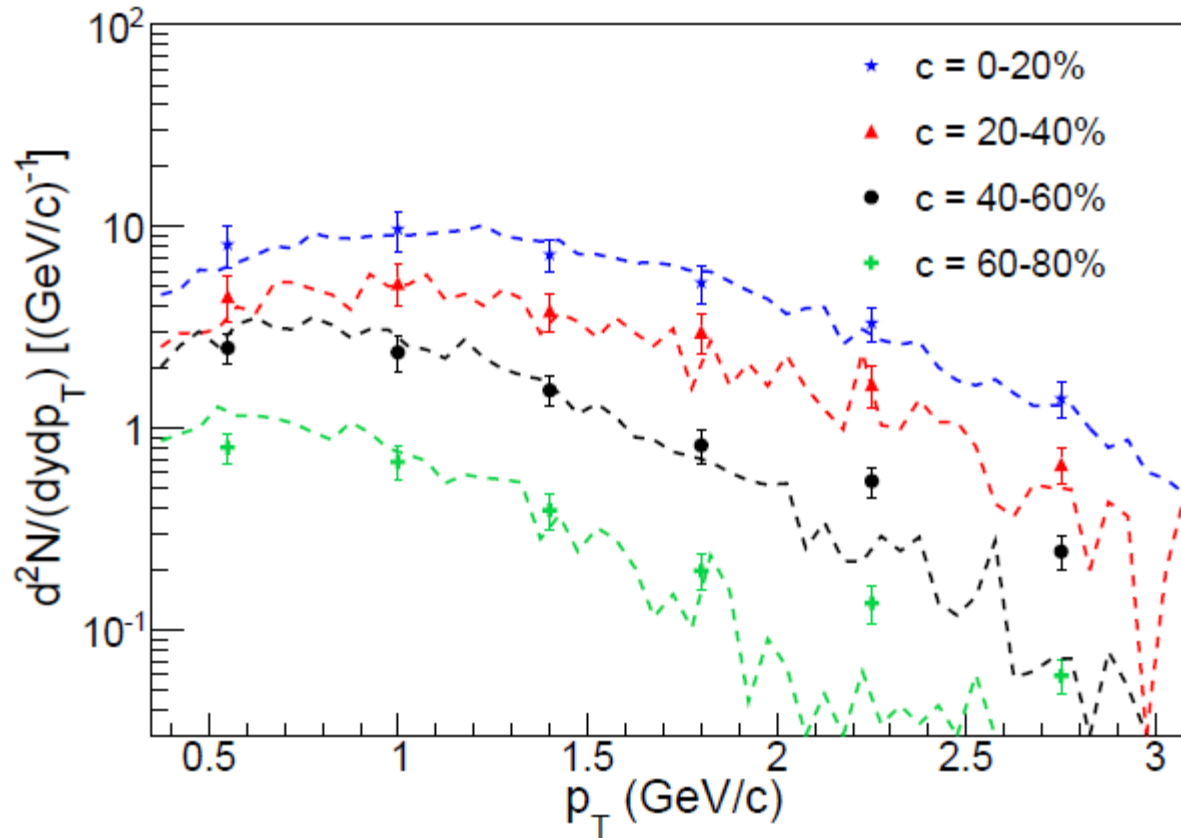
The comparison of K^*/K^+ and ϕ/K^+ ratios dependency on particle multiplicity $(dN_{ch}/d\eta)^{1/3}$ calculated in iHKM for the case of LHC Pb+Pb collisions at $\sqrt{s_{NN}} = 2.76$ TeV and the corresponding ALICE experimental data [6]. The solid lines correspond to the iHKM calculations, performed using hadronization temperature $T_{sw} = 163$ MeV and Laine-Shroeder equation of state [15], while the dashed lines are related to the Karsch equation of state [16] and $T_{sw} = 156$ MeV.

Ratios to K (RHIC)



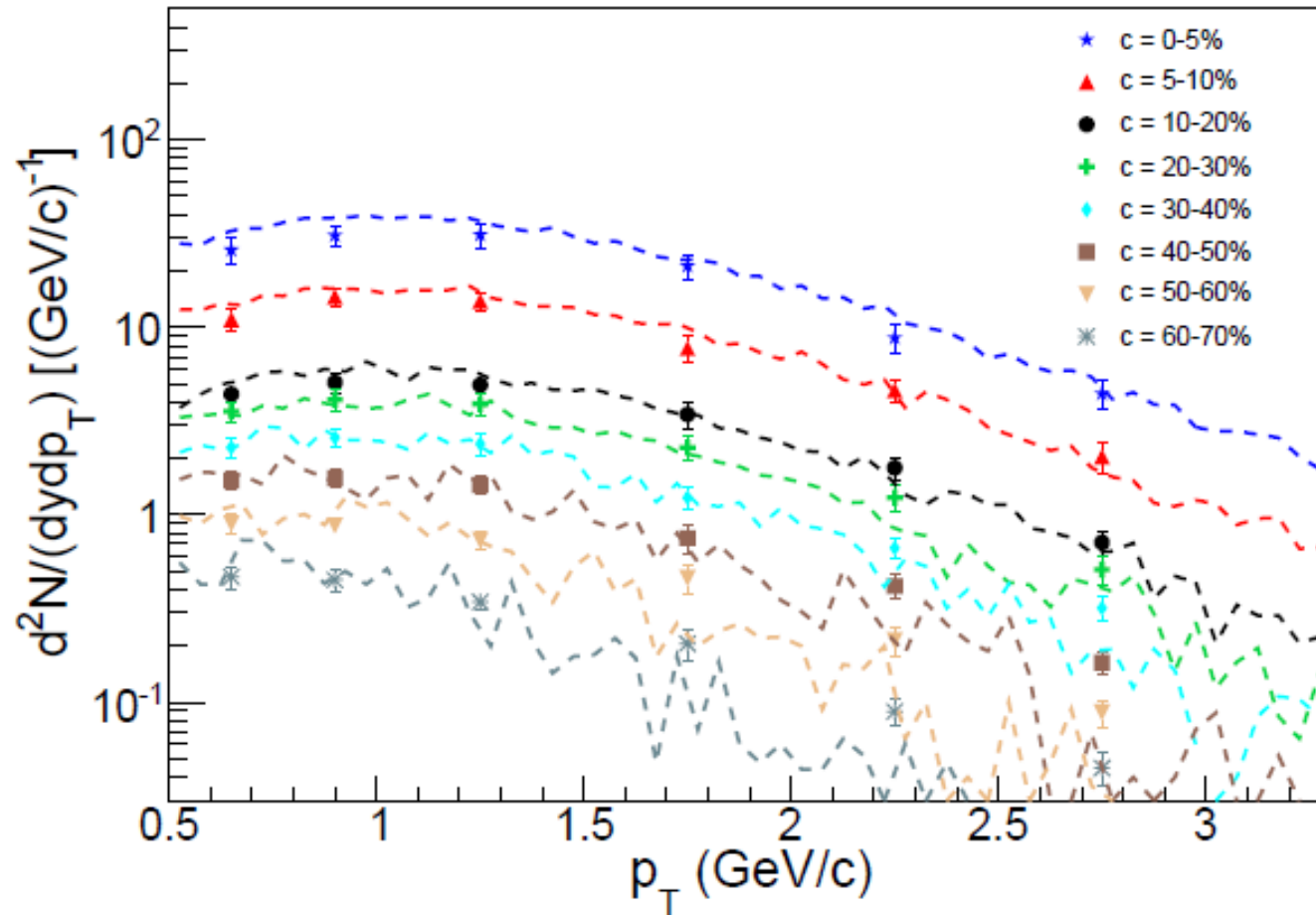
The comparison of K^*/K^+ ratio calculated in iHKM for the case of RHIC Au+Au collisions at $\sqrt{s_{NN}} = 200$ GeV and the experimental data [7] for different centrality classes.

Spectra of K^{*0} (LHC)



The $K(892)^*$ resonance p_T spectra for Pb+Pb collision events with different centralities at the LHC energy $\sqrt{s_{NN}} = 2.76$ TeV obtained in iHKM simulations (lines) in comparison with the experimental data [6] (markers).

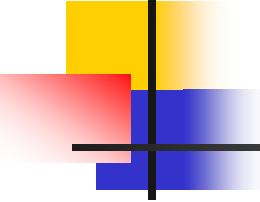
Spectra of ϕ (LHC)



The $\phi(1020)$ resonance p_T spectra for Pb+Pb collision events with different centralities at the LHC energy $\sqrt{s_{NN}} = 2.76$ TeV obtained in iHKM simulations (lines) in comparison with the experimental data [6] (markers).

Summary on the particle production

- Neither thermal nor chemical freeze-out cannot be considered as sudden at some corresponding temperatures.
- Particle yield probe $\frac{dN_i}{d\eta} / \frac{dN_j}{d\eta}$ as well as absolute values $\frac{dN_i}{d\eta}$ (!) demonstrate that even at the minimal hadronization temperature $T_{ch} = T_h = 156$ MeV, the annihilation and other non-elastic scattering reactions play role in formation particle number ratios, especially.
- It happens that the results for small and relatively large T_h are quite similar. It seems that inelastic processes (other than the resonance decays), that happen at the matter evolution below T_h play a role of the compensatory mechanism in formation of $\frac{dN_i}{d\eta} / \frac{dN_j}{d\eta}$.
Chemical freeze-out is continuous.
- As for the thermal freeze-out, the $K^{*0}(892)$ probes demonstrate that even at the first 4-5 fm/c (proper time!) after hadronization **at least** 70% of decay products are re-scattered. The intensive re-generation of K^* takes place. **At least** 50% of direct $K^{*0}(892)$ are re-combine.
- About 30% of much longer-lonq-lived resonances $\phi(1020)$ with hidden strange quark content created additionally to direct $\phi(1020)$ (coming from hadronization) at the afterburner stage.



Conclusion

To study the matter properties using the strange meson probes at the FAIR and NICA accelerators one needs:

EXPERIMENT

To provide the measurements of

total multiplicity vs centrality,
pion and kaon spectra,
comparative analysis of the femtoscopy radii behavior for pions and kaons,
particle number ratios in central events,
 K^*/K and ϕ/K ratios vs centrality

THEORY

To develop full evolutionary model:

initial state \rightarrow pre-thermal stage \rightarrow 3D thermal or quasi-thermal expansion of continuous medium (EoS - ?) \rightarrow particlization \rightarrow expansion of interacting hadron-resonance gas.

One of the candidates is iHKM, transformed for reach baryon matter

Thank you for your attention !